ME-88-10

Optimizing Infrared Detection for Bridge Deck Deterioration

Ontario

Ministry of Transportation

Research and Development Branch

Technical Report Documentation Page

Optimizing Infrared Detection for Bridge Deck Deterioration

Author(s):	T. Masliwec, Research Scientist, Materials Research Office, Research and Development Branch
Number:	MF-88-10
Date of Publication:	April 1990
Ministry Contact:	Tony Masliwec (416) 235-4689
Abstract:	Infrared thermography is used in non-contact, non-destructive testing of bridge decks for deterioration. The thermographic images, in mapping the ambient temperature levels of the surveyed deck, identify areas of relative heat concentration that correlate well with subsurface delaminations in the deck. While the system is capable of mapping such deterioration in exposed or asphalt covered decks, operational limitations, due to the weather conditions in the province, inhibit its year-round use. This report describes research studies which were undertaken to develop 1) theoretical heat transfer model for different types of bridge deck; 2) assess the validity of the theoretical model by collecting field data and performing correlation tests; 3) provide guidelines for the application of the infrared imaging system relative to the ambient conditions at test sites.
Comments:	Final report of Research and Development Branch project 22168
Key words:	DART, infrared, heat transfer, bridge deck, thermocouple
Distribution:	Structural Engineers
Copyright Status:	Crown copyright © 1988

Optimizing Infrared Detection for Bridge Deck Deterioration

T. Masliwec
Research Scientist
Materials Research Office
Research and Development Branch

Published by
The Research and Development Branch
Ontario Ministry of Transportation
Hon. Ed Fulton, Minister
D.G. Hobbs, Deputy Minister

Published without prejudice as to the application of the findings.
Crown copyright reserved; however, this document may be reproduced for non-commercial purposes with attribution to the Ministry.

For additional copies, contact:
The Editor, Technical Publications
Room 320, Central Building
1201 Wilson Avenue
Downsview, Ontario
Canada M3M 1J8

Telephone: (416) 235-3480
CNCP Dialcom Electronic Mail: 23:MIN006

April 1990

Table of Contents

1/ Introduction 1

2/ Heat Exchange and Thermal Effects 4
2.1/ Heat Transfer by Radiation 4
2.2/ Heat Transfer by Conduction and Convection 6
2.3/ Heat Transfer by Conduction, Convection, and Radiation Combined 7

3/ Thermal Properties of Concrete 8
3.1/ Thermal Conductivity 8
3.2/ Thermal Diffusivity 8
3.3/ Specific Heat 8
3.4/ Overall Heat Energy Exchange 9

4/ Theory 10
4.1/ Bridge Deck Heat Transfer Model 22

5/ Experimental Results 26
5.1/ Measurement of Temperature 26
5.2/ Measurement of Sun and Shade Temperature 27
5.3/ Recording of Temperature 28
5.4/ Experimental Data 28
5.5/ IR Observations 29
5.6/ Thermocouple Data From Asphalt Covered Decks 30

6/ Summary 33

7/ Comments and Recommendations 39

8/ References 40

Table and Figures

Tables

Table 1/ 43
Table 2/ 44

Figures

Figure 1/ 45
Figure 2/ 45
Figure 3/ 46
Figure 4/ 46
Figure 5/ 47
Figure 6/ 47
Figure 7/ 48
Figure 8/ 48
Figure 9/ 49
Figure 10/ 49
Figure 11/ 50
Figure 12/ 50
Figure 13/ 51
Figure 14/ 51
Figure 15/ 52
Figure 16/ 52
Figure 17/ 53
Figure 18/ 54
Figure 19/ 55
Figure 20/ 55
Figure 21/ 56
Figure 22/ 56
Figure 23/ 57
Figure 24/ 57
Figure 25/ 58

1/ Introduction

Research conducted at MTO has shown that infrared thermography obtained from a van-mounted system is a viable non-destructive and non-contact remote sensing tool for detecting deterioration in bridge decks. The thermographic images in mapping temperature (energy) levels of a surveyed deck, identify areas of relative heat concentration which correlate well with sub-surface deterioration in the deck.

The infrared detection of deteriorated areas in bridge decks is based upon the difference in surface temperature, which exists between deteriorated and sound concrete under certain atmospheric conditions. The surface temperature differences develop as a result of different rates of heat transfer inward from the surface. The surface, while being illuminated by the sun, is presumed to receive a uniform heat flux. The heat is conducted from the surface inward to the mass of concrete and reinforcing material constituting the bridge structure. Anything which impedes the conductive heat flow from the surface will result in a higher surface temperature. An explanation of this effect is based on the concept that delaminated areas are filled with "dead air" thus acting as insulating barriers which retard the conduction of heat away from the surface and hence lead to higher surface temperatures. (Conversely, uninterrupted areas will have lower surface temperatures.)

At night, the situation is reversed. The surface loses heat by radiation. This heat is supplied by conduction from the heated mass of the bridge. Any insulating layer which impedes that conduction will therefore cause a lowering of the surface temperature. Consequently, since heat is not replaced as rapidly as it is lost, the areas overlying delaminations will be cooler than the surrounding solid sections. These surface temperature differences have been detected by IR thermography when the defect occurs near the surface, well below the surface, and covered with asphalt overlay.

Temperature differences in bridge decks have also been studied by implanting thermocouples into the surface for direct temperature measurement and more extensively, by the use of infrared imaging for the measurement of surface radiance.

Temperature differences experimentally monitored ranged from 0.2°C to 9.0°C depending on the time of day, the severity of the defect, and the type of surfacing. The highest temperature differences always occur in direct sunlight on unsurfaced concrete decks. From the large number of thermographic studies reported there is little doubt as to the ability of infrared imaging to detect delaminated areas.

The infrared system used in the Deck Assessment by Radar and Thermography (DART) prototype has a sensitivity range of 3.0 to 5.6 microns and utilizes an Indium Antimonide (InSb) detector, with a sensitivity of 0.1°C. Using a 20° lens, the system is capable of scanning an entire traffic lane width in a single pass. The scanner (mounted 5 metres above the ground at an oblique angle of 45°) is connected through a control unit to a proprietary interface unit which converts the scanner signal to a standard NTSC video signal.

The output of a 5th wheel is recorded on an audio channel of a VCR. This enables a microcomputer to process the IR data and identify the longitudinal position of the scanner on the deck. Data can be collected at up to 6 km/h, beyond which speed, motion smear distorts the image. Software for a microcomputer has been developed to analyze the infrared image. First, the video tape is digitized and then it is sampled in such a way that the oblique angle of view and other distortions of the image are eliminated.

Defects are identified through a combination of operator and machine interpretation. The software produces a scaled hardcopy image of the bridge deck showing areas of deterioration. While the infrared system is capable of mapping deterioration in bridge decks, operational limitations due to environmental conditions encountered in the Province, inhibit its year round use. Since the infrared system measures differences in emitted surface energy, the distinction between sound and unsound concrete was expected to be most visible during periods of rapid heating and cooling. During the day, it was found that solar radiation on the bridge deck was effective in raising the surface temperature almost immediately (by 9:00 am in the summer - see Experimental section), creating temperature differentials which enabled the areas of sound and unsound concrete to be distinguished. The longer the period of solar radiation, the greater the temperature differentials became and the clearer the deterioration was defined. During the course of this work, temperature differentials were found to stabilize between 1.5°C and 4.5°C.

Although the infrared scanner has a sensitivity of 0.1°C, higher differentials are desirable to counteract the effect of differences in deck emissivity due to such factors as wheel polishing, oil stains, or debris. Ambient temperatures ranging from -32°C to 32°C were not found to have an effect on the detectability of deterioration, since, it is temperature differentials which are important in deck condition surveys not absolute temperatures. However, the differentials were greater in the summer because of the greater intensity of solar radiation and the prevalence of drier deck surfaces (no snow).

The objectives of this study are to:

1) Compare observed infrared data with a theoretical heat transfer model for bridge decks.
2) Assess the validity of the theoretical model by collecting field data and performing correlation tests.
3) Define the range of ambient conditions within which the infrared system can be operated with predictable reliability.
4) Implement necessary adjustments and modifications to the system to facilitate its application over an acceptable range of ambient conditions.
5) Recommend modifications to the processing software for any additional requirements identified in this study.

2/ Heat Exchange and Thermal Effects

Any structure exposed to the atmosphere is subject to an exchange of heat energy at its surface, to and from its surrounding environment. A bridge is continually losing or gaining heat, the amount and rate of which is dependent on many elements. These are:

1) convection to or from the surrounding atmosphere,
2) radiation to or from the sky and surrounding objects, and
3) radiation from the sun.

Temperature changes which are a result of these sources depend on a number of factors such as:

1) latitude of locality,
2) time of day and season,
3) orientation of bridge deck to the sun,
4) degree of cloudiness and relative humidity,
5) nature and colour of bridge deck surface,
6) thermal properties of constituent materials of the bridge.

2.1/ Heat Transfer by Radiation

Heat transfer by radiation is considered to be the mechanism of most importance. During the daylight hours, when a bridge is exposed to the sun, there is a net gain in the heat energy of the structure. This net gain is mainly a result of the absorption of solar radiation by the structures surface. During the night however, the converse occurs primarily as a result of re-radiation to the surrounding environment of the heat energy stored in the structure. In the case of heat energy input, the intensity of the solar radiation reaching the earth's atmosphere is dependent on the distance between the earth and the sun. The intensity also depends on the length of daylight time, latitudinal variations, and several other factors (see Figure 1) pertaining to the conditions within the earth's atmosphere. (The variation of solar radiation with latitude is shown in Figure 2.)

The radiation impinging on the surface of the bridge may be categorized into two basic types; longwave and shortwave radiation. Shortwave radiation (wavelength 2 to 6 microns) impinges on a bridge deck directly from the sun (with a minor contribution due to diffuse radiation from the sky – also known as indirect solar radiation). Shortwave radiation may be weakened by cloud formations and the earth's atmosphere, and it can be reflected by the bridge and its surroundings. The actual amount of solar radiation incident on the bridge deck is dependent on the inclination and orientation of the surface to the sun.

Longwave radiation (wavelength 6 to 60 microns) is emitted from any object as a result of its own stored heat energy. Heat exchange by longwave radiation is secondary in importance to heat exchange by shortwave radiation. However, at night it can account for significant exchanges of heat energy at the deck surface. In certain cases, heat loss by longwave radiation can result in night-time surface temperatures (on a solid bridge deck) being lower than those of the surrounding air. During daylight hours, longwave radiation also adds to the heat energy input of a bridge deck; the quantity received is dependent on the inclination of the surface to the horizontal.

The actual radiation heat exchange is complex and therefore simplifying approximations must be made. A comprehensive equation governing the solar heat energy input at the upper surface of a bridge deck is assumed. It is also assumed that the exchange of heat energy takes place in the vertical direction only; the assumption is generally valid since the depth is usually small compared with the plan dimensions. An equation giving an approximation to the daily variation of radiation impinging on a horizontal surface is developed as follows:

For a given latitude and solar declination, global radiation on a horizontal surface is broadly a function of solar attitude which in turn is a function of cos H, where H is the local hour angle (see Figure 3). If we let:

$G(t)$ = intensity of global radiation on a horizontal surface at time t (measured from sunrise)

$G(x)$ = intensity at local apparent noon and assumed to be maximum for the day

T = day length

t = time from sunrise of solar radiation

S = daily integral solar radiation and equal to the area under the curve

α = t/T $(0 \leq t \leq T)$

Then, with the origin at sunrise (see Figure 3),

$$G(t) = G(x) \sin \alpha - \alpha$$

Integrating from 0 to T we obtain;

$$S = G(x) \frac{2T}{\pi}$$

and hence $G(t) = \frac{S\pi}{T2} \sin \frac{\pi t}{T}$

The radiation, which finally impinges on the surface shown in Figure 1, has two primary effects. It may penetrate the surface, be absorbed and converted to heat, or it may be reflected. If the amount which is absorbed and converted to heat is defined as Q and that which is reflected is R, then for a unit amount of radiation heat energy: $1 - Q = R+C$, where C is the transmissivity of the medium or the amount of radiation which passes through the medium without being absorbed. In the case of concrete, C is equal to zero.

Various media absorb different quantities of radiation. Colour bodies are distinguished by their selective absorption of different wavelengths of light. A body which is a perfect absorber of all wavelengths of light (as well as a perfect emitter of all wavelengths) is defined as a blackbody. Concrete structures function as grey bodies, since they absorb a certain amount of all wavelengths and reflect the remainder.

In the case of bridges, the type of surfacing has a significant impact on the amount of radiation absorbed. Several authors (Emerson, Priestly, Kehlbeck) have investigated the effect of a white surfacing, a black surfacing, and plain (exposed) concrete surfaces. They discovered that the surface temperatures of concrete were highest when the deck was unsurfaced. A white surfacing was found to give the lowest temperatures, and a black surfacing yielded temperatures in the concrete which were about 10% lower than those occurring in the unsurfaced condition. The latter result was due to the insulating effect of the blacktop layer, even though it has a greater absorptivity of radiation than the unsurfaced concrete.

2.2/ Heat Transfer by Conduction and Convection

In addition to heat transfer by radiation, heat transfer by conduction and convection also take place at a bridge deck surface. However, heat transfer by conduction alone is small and difficult to assess. Therefore, it is normal (Barber, Zuk, Emerson) to allow for heat transfer due to conduction and convection by assuming a combined heat transfer coefficient, which is sensitive to wind velocity, ambient air temperature, and surface temperature. Since wind velocities are difficult to predict, values for the combined coefficient are not easily obtained. Often, monthly averages of temperature and wind velocity are used.

2.3/ Heat Transfer by Conduction, Convection, and Radiation Combined

A certain amount of heat energy exchange also takes place due to the re-radiation of the structure and its surroundings. As mentioned previously, this type of heat exchange is generally in the form of longwave radiation. (The IR scanner used with the DART system is not very sensitive at the longer wavelengths and consequently, is not seriously impeded by this emitted wavelength range). In order to simplify the heat transfer model, an overall heat transfer coefficient which combines heat transfer by conduction, convection, and radiation is generally adopted.

3/ Thermal Properties of Concrete

3.1/ Thermal Conductivity

This measures the ability of the material to conduct heat and is defined as the ratio of the flux of heat to the temperature gradient. Thermal conductivity is measured in joules per second square metre of area of body (BTU/h/ft^2 when the temperature difference is 1°F per ft. of thickness).

The conductivity of ordinary concrete depends on its composition. When it is saturated, the conductivity generally ranges between approximately 1.4 and 3.6 Jm^{2}s°C/m (0.8 and 2.1 BTU/ft^{2}h°F/ft). Density does not appreciably affect the conductivity of concrete but, due to the low conductivity of air, the thermal conductivity of lightweight concrete varies with its density. (Typical values are listed in Table 1). From Table 1, it can be seen that the mineralogical composition of the aggregate greatly affects the conductivity of the concrete.

The degree of saturation of concrete is a major factor since the conductivity of air is lower than that of water. For instance, in the case of lightweight concrete, an increase in moisture content of 10% increases conductivity by about one half. A practical difficulty is to estimate the actual moisture content of the concrete. For this reason, values of conductivity are given in Table 2.

3.2/ Thermal Diffusivity

Diffusivity represents the rate at which temperature changes within a mass can take place and is therefore an index of the facility with which concrete can undergo temperature changes. Diffusivity, D, is related to conductivity, K, by the equation: $D = \frac{K}{CQ}$, where C is the specific heat and Q is the density of the concrete. From this expression, it can be seen that conductivity and diffusivity vary linearly with each other.

3.3/ Specific Heat

Specific heat, which represents the heat capacity of concrete, is negligibly affected by the mineralogical composition of the aggregate, but is considerably affected by any change in the moisture content of the concrete. Specific heat increases with an increase in temperature and a decrease in the density of the concrete. The common range of values for ordinary concrete is

between 840 and 1170 J/kg/°C (0.20 and 0.28 BTU/lb/°F). The specific heat of concrete is determined by elementary methods of physics.

3.4/ Overall Heat Energy Exchange

Once the variables governing the heat energy exchange have been defined and quantified, the expression governing the surface boundary conditions is developed in order that surface temperatures and profiles may be calculated. A bridge deck is continually gaining and losing heat which produces both seasonal and diurnal variations in the bridge. The temperature distribution through a bridge deck depends on the local weather conditions as well as section depth and the thermal properties of the concrete. As previously described, the basic quantities that determine the thermal behaviour of concrete are thermal conductivity, thermal diffusivity, and specific heat. These properties vary widely for typical bridge decks and are a function of the composition of the mix, degree of saturation, and mineralogical composition of the aggregate used.

4/ Theory

Prior to deriving a quantitative heat transfer model for a bridge deck, several assumptions must be made. These are:

1) Surface heat transfer coefficients remain constant throughout the time period of concern.
2) Thermal properties of the bridge deck are independent of the temperature variation.

Once the external parameters governing the heat energy exchange at the surface of a bridge have been evaluated, the boundary conditions can be calculated for any instant in time. A knowledge of the boundary conditions enables the non-linear temperature distribution throughout the structure (and at the surface) to be calculated. This non-linear distribution is due to the poor thermal conductivity of concrete and to the constantly changing external conditions. That is, for the majority of bridges, the vertical heat flow through the thickness is of greater significance than transverse heat flow since the depth is usually small compared with the plan dimensions. This means that actual heat flow can be represented realistically by one-dimensional heat transfer theory. The material properties which govern the flow of heat through a body are density, thermal conductivity, and specific heat (ρ , k, and c, respectively).

The rate at which heat is transferred across any surface at a point per unit area per unit time is called the flux of heat across the surface at that point and can be denoted by f.

The value of the flux will depend on the position of the point, the direction of the normal to the surface at the point, and the time. Looking at an infinitesimal area (a) in the figure below and enclosing P in a plane,

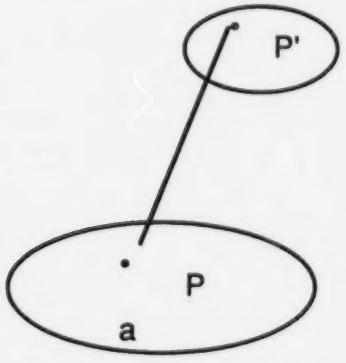

a cylinder is formed on this area as a base with generators equal and parallel to a line PP', whose length (l) is an infinitesimal of lower order than the linear dimension of a.

Let f_1a and f_2a be the rates of flow per unit time across the plane surfaces of the cylinder through P and P'. The flow across the curved surface is negligible compared with these. The rate of flow of heat into the cylinder is thus a (f_1-f_2). Also, if T is the average temperature in the cylinder, d the distance between its plane faces, and ρ and c the average density and specific heat of the material, the rate at which the cylinder gains heat is $\frac{\rho\, dcl\partial T}{\partial t}$ or, equating the two expressions, gives $f_1-f_2 = \frac{\rho\, dcl\partial T}{\partial t}$ and as $d \rightarrow 0$ the expression on the right tends to zero, hence f_1 approaches f_2. (The preceding argument does not require the thermal properties of the medium to be continuous, only that they be finite.)

It should be noted at this point, that only isotopic structures will be considered. (That is, bridges whose structure and properties in the neighbourhood of any point are the same relative to all directions through that point.) Due to this symmetry, the flow of heat at a point must be normal to the isothermal surface through the point and in the direction of falling temperature. In the previous diagram, isotherms would be planes parallel to the faces of the cylinder. If the isotherms for temperatures T and T + dT are a distance dx apart, then the rate of flow of heat per unit time per unit area in the direction of increasing x is $-k\frac{dT}{dx}$ and as $dx \rightarrow 0$, we have $fx = -k\frac{dT}{dx}$ If this is now extended to any isothermal surface and taken as a fundamental hypothesis for the theory of conduction of heat (Sears, Salinger), then the rate at which heat crosses from the inside to the outside of a surface per unit area per unit time at a point is equal to $-k\frac{dT}{dn}$, where k is the thermal conductivity of a substance and $\frac{d}{dn}$ denotes differentiation along the outward bound normal to the surface.

Before the mathematical discussion of heat flow in a bridge deck may proceed, it is necessary to determine the formulae which will express the initial and boundary conditions which the temperature satisfies.

We assume that the interior of the deck, T, is a continuous function of x, y, z and t and that this also holds true for the first differential coefficients with regard to t (time) and the first and second differential coefficients with regard to x, y, and z. At the boundary of the bridge deck, and at the instant which the flow of heat is supposed to start, these assumptions are not valid.

The temperature throughout the body is given arbitrarily at the instant which we take as the origin of the time component t. If this arbitrary function is continuous, we are required to find a solution to our problem which shall, as t tends to zero, tend to the given value. In other words, if the initial temperature is given by T = f(x, y, z), a solution of the equation $\frac{\partial T}{\partial t} - k \nabla^2 T$ must be such that lim T = f(x,y,z) at all points in the deck (Carrier and Pearson).

If the flux across the deck surface is proportional to the temperature difference between the surface and the surrounding medium, so that it is given by $H(T-T_o)$, where T_o is the temperature of the medium and h is a constant called the surface coefficient, the boundary condition is

$$k\frac{dT}{dn} + H(t-t_0) = 0 \text{ or } \frac{dT}{dn} + h(T-T_0) = 0, \text{ where } H = \frac{h}{k}$$

In the mathematical treatment, the boundary and initial conditions are not regarded as conditions which the temperature T must satisfy at the surface itself or at the instant t = 0. Rather, they are taken as limiting conditions.

The boundary conditions are understood in the sense that, for fixed t > 0, the given combination of the temperature and its derivatives is to tend to the prescribed value as a point on the surface is approached. The initial conditions are understood in the sense that, for a fixed point within the region of interest, the temperature is to tend to the prescribed value as t approaches 0 in its limit.

When the surface condition varies with time, or when radiation takes place at the surface of a bridge deck whose temperature varies with time, the solution to the general heat diffusion equation becomes more difficult. One solution to the problem may be referred to as Duhamel's method (Carslaw and Jaeger) which depends on the following theorem:

> If T = f(x,y,z,λ,t) represents the temperature at (x, y, z) at the time, t, in a solid in which the initial temperature is a constant throughout, while its surface temperature is $\phi(\lambda)$, then the solution of the problem in which the initial temperature is constant and the surface temperature is $\phi(x,y,z,t)$ is given by:

$$T = \int_0^t \phi(\lambda) \frac{\partial}{\partial t} F(x,y,z,\lambda,t-\lambda)d\lambda \qquad (1)$$

For the case where $\frac{dT}{dt} = k \nabla^2 T$ through the deck, (2)

$T = f(x,y,z)$ initially

$T = \phi(x,y,z,t)$ at the surface

we let $T = u + w$ which reduces (2) to

$\frac{du}{dt} = k \nabla^2 u$ through the deck, (3)

$u = 0$ initially

$u = (x,y,z,0)$ at the surface

and $\frac{dw}{dt} = k \nabla^2 w$ through the deck, (4)

$w = f(x,y,z)$

$w = 0$ at the surface

Hence, using Duhamel's method, the problem is simplified to the case of surface temperature which is independent of time. Problems with other boundary conditions may be reduced in the same way (Carslaw and Jaeger).

In the theoretical case where a solid is unbounded and the initial temperature is given by $T = f(x)$, the equation of condition (2) reduces to $\frac{\partial T}{\partial t} = k \frac{\partial T^2}{\partial x^2}$ (5) since T depends on only x and t. This is a condition we find for the majority of bridges since the vertical heat flow through the thickness of a bridge is of greater significance than the transverse heat flow. (This is because the depth is usually small compared with to the plan dimensions.)

Consider the expression, $u = \frac{1}{\sqrt{t}} e^{-x^2/4kt}$

Since $\frac{du}{dt} = \frac{-1}{2t^{3/2}} e^{-x^2/4kt} + \frac{x^2}{4kt^{5/2}} e^{-x^2/4kt}$

and $\frac{d^2u}{dx^2} = \frac{1}{2kt^{3/2}} e^{-x^2/4kt} + \frac{x^2}{4k^2t^{5/2}} e^{-x^2/4kt}$

this expression is a particular integral of the differential equation.

Therefore $\frac{1}{2\sqrt{\pi kt}} \int_{-\infty}^{\infty} f(x') \, e^{-(x-x')^2/4kt} \, dx'$ is also an integral. Further, since the equation is linear, the sum of any number of particular integrals is also an integral, thus:

$$T = \frac{1}{2\sqrt{\pi kt}} \int_{-\infty}^{\infty} f(x') \, e^{-(x-x')^2/4kt} \, dx'$$

satisfies the equation, assuming that this integral is convergent. Setting $x' = x + 2\sqrt{kt}\,\xi$ we find that:

$$T = \frac{1}{\sqrt{\pi}} \int_{-\infty}^{\infty} f(x + 2\sqrt{kt}\,\xi) \, e^{-\xi^2} \, d\xi$$

In the limit when $t \to f(x + 2\sqrt{kt}) = f(x)$, if this function is continuous; and it is assumed that the limiting value of this integral is given by $\frac{1}{\sqrt{\pi}} \int_{-\infty}^{\infty} f(x) \, e^{-\xi^2} \, d\xi$ which is equal to f(x). Therefore, the temperature in the infinite solid at time t, due to the initial temperature T = f(x), is given by:

$$T = \frac{1}{2\sqrt{\pi kt}} \int_{-\infty}^{\infty} f(x') \, e^{-(x-x')^2/4kt} \, dx' \qquad (6)$$

If we let the solid be bounded by a plane at x = 0 and extend to infinity in the direction of x negative, the initial temperature given by T = f(x) and the plane x = 0 at zero temperature then the solution of this problem may be deduced from that of the infinite solid.

We suppose the solid continued on the positive side of the plane x = 0, and the initial temperature at x' (x' > 0) to be -f(x'), the initial temperature at x' being f(x'). With this distribution, the plane x = 0 will remain at zero. Thus from (6):

$$T = \frac{1}{2\sqrt{\pi kt}} \left\{ \int_{0}^{\infty} f(x') \, e^{-(x-x')^2/4kt} \, dx' + \int_{-\infty}^{\infty} -f(-x') \, e^{-(x-x')^2/4kt} \, dx' \right\}$$

$$= \frac{1}{2\sqrt{\pi kt}} \int_0^\infty f(x') \, e^{-(x-x')^2/4kt} - e^{-(x-x')^2/4kt} \, dx' \qquad (7)$$

It is clear that this value of T satisfies all the conditions of the problem of the semi-infinite solid whose boundary plane is kept at zero temperature. This may be transformed into:

$$T = \frac{1}{\pi} \int_0^\infty dx' \int_0^\infty f(x') \, [\cos(x - x') - \cos \partial(x' + x) \, e^{-k\alpha^2 t} \, d\alpha \,]$$

$$= \frac{2}{\pi} \int_0^\infty dx' \int_0^\infty f(x') \sin \alpha x' \sin \alpha \, x \, e^{-k^2 t} \, d\alpha \,]$$

a form suggested by Fourier's sine integral (Carrier and Pearson).

When the initial temperature is a constant V, the expression (7) may be simplified by substituting $x' = x + 2\xi\sqrt{kt}$ in the first part; and $x' = -x + 2\xi\sqrt{kt}$ in the second. Obtaining:

$$T = \frac{V}{\sqrt{\pi}} \int_{\frac{-x}{2\sqrt{kt}}}^{\frac{x}{2\sqrt{kt}}} e^{-\xi^2} \, d\xi = \frac{2V}{\sqrt{\pi}} \int_0^{\frac{x}{2\sqrt{kt}}} e^{-\xi^2} \, d\xi$$

Integrals of this type have been tabulated (CRC handbook), and if we write:

$$\text{erf}(x) = \frac{2}{\sqrt{\pi}} \int_0^x e^{-\xi^2} \, d\xi \quad [\text{also erfc}(x) = 1 - \text{erf}(x)],$$

the solution of the problem of the semi-infinite solid, whose surface is kept at zero temperature, the initial temperature being V, is given by:

$$T = V \, \text{erf}\left(\frac{x}{2\sqrt{kt}}\right) \qquad (8)$$

In the case of constant initial temperature V and zero surface temperature, the result depends on the single dimensionless parameter $\frac{x}{2\sqrt{kt}}$. This makes it easy to compare temperatures at different

times and places in solids of different conductivity. Similar results hold for the rate of cooling and the temperature gradient at any point, both of which are often needed. The rate of cooling at any point is:

$$-\frac{\partial T}{\partial t} = \frac{Vx}{2\sqrt{\pi kt}} e^{-(x^3/4kt)}$$

The temperature gradient at any point is: $\frac{\partial T}{\partial x} = \frac{V}{\sqrt{\pi kt}} e^{-(x^2/4kt)}$

Thus, in terms of the parameter $x/2\sqrt{kt}$ we have:

$$\frac{T}{V} = \text{erf}\left(x/2\sqrt{kt}\right) = \frac{-t\sqrt{\pi}}{V}\frac{\partial T}{\partial x} = \frac{x\sqrt{\pi}}{2V}\frac{\partial T}{\partial x} = \frac{x}{2\sqrt{kt}} e^{-(x^2/4kt)} \tag{9}$$

If the boundary x = 0 is kept at constant temperature V and initial temperature is zero from (6):

$$T = V\left(1 - \text{erf}\,\frac{x}{2\sqrt{kt}}\right) = V\text{erfc}\left(x/2\sqrt{kt}\right) \tag{10}$$

We have seen earlier that when the surface temperature varies with the time, the solution may be derived, by Duhamel's theorem, from the case in which this temperature is constant. Now, in the semi-infinite solid, where T has to satisfy:

$$\frac{\partial T}{\partial T} = k^2\frac{\partial^2 T}{\partial x^2}$$

$T = 0$ when $t = 0$

$T = 1$ at $x = 0$

and the solution, given by (10) is:

$$T = 1 - \frac{2}{\sqrt{\pi}} \int_0^{\frac{x}{2\sqrt{kt}}} e^{-\xi^2}\, d\xi = \frac{2}{\sqrt{\pi}} \int_{\frac{x}{2\sqrt{kt}}}^{\infty} e^{-\xi^2}\, d\xi$$

Therefore, if:

$$\frac{\partial T}{\partial t} = \frac{k\partial^2 T}{\partial x^2}$$

$$T = 0 \text{ for } t = 0$$

$$T = \phi(t) \text{ for } x = 0$$

it follows from Duhamel's theorem that:

$$T = \int_0^t \phi(\lambda) \frac{d}{dt} F(x,t-\lambda)\, d\lambda$$

where $F(x,t-\lambda) = \frac{2}{\sqrt{\pi}} \int_{\frac{x}{2\sqrt{k(t-\lambda)}}}^{0} e^{-\xi^2} d\xi$

In this case,

$$\frac{\partial}{\partial t} F(x,t-\lambda) = \frac{-2}{\sqrt{\pi}} e^{-x^2/4k(t-x)} \frac{d}{dt}\left[\frac{x}{2\sqrt{k(t-\lambda)}}\right] = \frac{x}{2\sqrt{\pi k(t-\lambda)^3}} e^{-x^2/4k(t-\lambda)}$$

Therefore from (8)

$$\phi(x,t) = \frac{2v}{\sqrt{\pi}} \int_0^{\frac{x}{2\sqrt{kt}}} e^{-\mu^2} d\mu$$

Therefore, the solution of the problem is:

$$T = \frac{x}{2\sqrt{\pi k}} \int_0^t \phi(\lambda) \frac{e^{-x^2/4k(t-\lambda)}}{(t-\lambda)^{3/2}} d\lambda$$

Setting $\frac{x}{2\sqrt{k(t-\lambda)}} = \mu$

we have $(t-\lambda) = \frac{x^2}{4K\mu^2}$

and

$$T = \frac{2}{\sqrt{\pi}} \int_{\frac{x}{2\sqrt{kt}}}^{\infty} \phi\left(t - \frac{x^2}{4K\mu^2}\right) e^{-\mu^2} d\mu \qquad (11)$$

We may solve the problem of the semi-infinite solid with initial temperature f(x) and surface temperature (t) by setting T = V + W,
where u satisfies

$$\frac{\partial u}{\partial t} = \frac{k\partial^2 u}{\partial x^2}$$

with u = 0 initially, and
u = ϕ(t), at x = 0, and
w satisfies $\frac{\partial w}{\partial t} = \frac{k\partial^2 w}{\partial x^2}$

with w = f(x), initially, and
w = 0 at x = 0

That is, u is the solution of the problem (11) and w is the solution as in (10).

If the surface temperature in semi-infinite solid x > 0 is given by T = A cos(wt-ε), the solution by (11) is

$$T = \frac{2A}{\sqrt{\pi}} \int_{\frac{x}{2\sqrt{kt}}}^{\infty} \cos\left(w\left(t - \frac{x^2}{4k\mu^2}\right) - \varepsilon\right) e^{-\mu^2} d\mu \qquad (12)$$

It is known that (Carslaw and Jaeger)

$$\frac{2}{\sqrt{\pi}} \int_0^{\infty} e^{-\mu^2} \cos\left(\frac{wx^2}{4k\mu^2} + \phi\right) du = e^{-\frac{x}{\sqrt{\frac{w}{2k}}}} \cos\left(x\left(\frac{w}{2k}\right)^{1/2} + \phi\right)$$

When t is so great that the lower limit of the integral in (12) may be taken to be zero, T is given by

$$T = A\ e^{-x\sqrt{w/2k}} \cos(wt\ - \varepsilon - x\left(\frac{w}{2k}\right)^{1/2}) \qquad (13)$$

This is the steady periodic solution which gives the temperature at all times, after the transient disturbance caused by starting the temperature oscillations at the surface has died away.

When the initial temperature is constant and equal to V, the equations for T are as follows:

$$\frac{dT}{dt} = \frac{kd^2T}{dx^2}$$
$$T = V_1 \text{ when } t = 0$$
$$-\frac{dT}{dx} + hv = 0 \text{ when } x = 0$$

Let $\phi = T\ \frac{1}{h}\ \frac{dT}{dx}$

Then we have $\frac{d\phi}{dt} = k\frac{d^2\phi}{dx^2}$

$$\phi = V \text{ when } t = 0$$
$$\phi = 0 \text{ when } x = 0$$

integrating this equation the usual way.

Therefore from (8)

$$\phi\ (x,t) = \frac{2V}{\sqrt{\pi}} \int_0^{\frac{x}{2\sqrt{kt}}} e^{-\mu 2}\ d\mu$$

and when $x \rightarrow \infty$, ϕ (x,t) has the limit V. To determine T we have the equation

$$\frac{dT}{dx} - hT = -h\phi\ (x,t)$$

Thus $T = (e^{hx} - he^{hx}) \int_{\infty}^{x} \phi(\xi,t)\, e^{-h\xi} d\xi$

on setting $\xi = x + \eta$. But as $x \to \infty$, $\phi(x,t)$ has the limit V, and T integrating this equation the usual way.

$$T = Ce^{hx} + h \int_0^{\infty} \phi(x + \eta, t) e^{-h\eta} d\eta$$

on setting $\xi = x + \eta$. But as $x \to \infty$, $\phi(x,t)$ has the limit V, and T must be finite, it follows that C must be zero. Hence the solution of the problem is given by:

$$T = h \int_0^{\infty} \phi(x + \eta, t)\, e^{-h\eta} d\eta = \frac{2Vh}{\sqrt{\pi}} \int_0^{\infty} e^{-h\eta} \left[\int_0^{\frac{(x+\eta)}{2\sqrt{kt}}} e^{-\mu^2} d\mu \right] d\eta$$

$$T = \frac{2V}{\sqrt{\pi}} \left[e^{-h\eta} \int_0^{\frac{x+\eta}{2\sqrt{kt}}} e^{-\mu^2} d\mu \right]_0^{\infty} + \frac{2V}{\sqrt{\pi}} \int_0^{\infty} e^{-h\eta} \frac{d}{d\eta} \left(e^{-\mu^2} d\mu \right) d\eta$$

$$= \frac{2V}{\sqrt{\pi}} \int_0^{\frac{x}{2\sqrt{kt}}} e^{-\mu^2} d\mu + \frac{V}{\sqrt{\pi kt}} \int_0^{\infty} e^{\frac{-h\eta - (x+\eta)^2}{\sqrt{4kt}}} d\eta$$

$$= \frac{2V}{\sqrt{\pi}} \int_0^{\frac{x}{2\sqrt{kt}}} e^{-\mu^2} d\mu + \frac{V}{\sqrt{\pi kt}} e^{hx + h^2kt} \int_0^{\infty} e^{-\frac{(x+\eta+2hkt)^2}{4kt}} d\eta$$

in the second integral set $x + n + 2hkt = 2\sqrt{kt}\mu$

Then, $T = \frac{2V}{\sqrt{\pi}} \int_0^{\frac{x}{2\sqrt{kt}}} e^{-\mu^2} d\mu + \frac{2V}{\sqrt{\pi}} e^{hx + h^2kt} \int_{\frac{x+2hkt}{2\sqrt{kt}}}^{\infty} e^{-\mu^2} d\mu$

$$= \frac{2V}{\sqrt{\pi}} \int_0^{\frac{x}{2\sqrt{kt}}} e^{-\mu}\, d\mu \; \frac{2V}{\sqrt{\pi}}\, e^{hx + h^2kt} \left(\int_0^{\infty} e^{-\mu 2}\, d\mu - \int_0^{\frac{x + 2hkt}{2kt}} e^{-\mu 2}\, d\mu \right)$$

Therefore:

$$\frac{T}{V} = \operatorname{erf}\left[\frac{x}{2\sqrt{kt}}\right] + e^{(hx + h^2kt)} \operatorname{erfc}\left[\frac{x}{2\sqrt{kt}} + h\sqrt{kt}\right] \qquad (14)$$

Where erfx and erfc(x) are as previously defined. (The surface temperature is obtained by letting x = 0 in (14).)

Our interest in this study lies in the case of a semi-infinite solid with radiation at the surface into a medium at temperature f(t) with initial temperature zero.

In this problem, the temperature (T) has to satisfy

$$\frac{\partial T}{\partial t} = k \frac{\partial^2 V}{\partial x^2}$$

$$- \frac{\partial T}{\partial x} + hT = hf(t) \quad \text{at } x = 0$$

$$T = 0 \text{ when } t = 0$$

Proceeding as in the last solution, let

$$\phi = T - \frac{1}{n} \frac{\partial T}{\partial x}$$

giving the following equations to determine ϕ.

$$\frac{\partial \phi}{\partial T} = k \frac{\partial^2 \phi}{\partial x^2}$$

$$\phi = f(t) \text{ at } x = 0$$

$$\phi = 0 \text{ when } t = 0$$

whose solution was given by (11), consequently

$$\phi = \frac{2}{\sqrt{\pi}} \int_{\frac{x}{2\sqrt{kt}}}^{\infty} f\left(t - \frac{x^2}{4k\mu^2}\right) e^{-\mu^2}\, d\mu$$

hence as in the development of (14)

$$T = \frac{2h}{\sqrt{\pi}} \int_0^{\infty} e^{-h\eta}\, d\eta \int_{\frac{x+\eta}{2\sqrt{kt}}}^{\infty} f\left(t - \frac{(x+\eta)^2}{4k\mu^2}\right) e^{-\mu^2}\, d\mu \qquad (15)$$

Similarly, in the case where f(t) = sin(wt + E) (which is the form of the problem we ultimately want to solve), from Carslaw and Jaeger we can show that:

$$T = \frac{h}{\sqrt{(h + w')^2 + (w')^2}} e^{-w'x} \sin(wt + E - w'x - \delta) +$$

(16)

$$\frac{2\ kh}{\pi} \int_0^{\infty} \left[\frac{(w \cos E - k\mu^2 \sin E)(\mu \cos \mu x + h \sin \mu x)}{(k^2\mu^4 + w^2)(h^2 + \mu^2)} \cdot e^{-k2\mu t} \right] \mu\, d\mu$$

where $w' = \sqrt{\frac{w}{2k}}$ and $\delta = \tan^{-1} \frac{w'}{h + w'}$. Since we are interested solely in a steady-state solution, only the first term applies to the bridge deck heat transfer problem.

4.1/ Bridge Deck Heat Transfer Model

Ideally, any semi-empirical approach should take into account such variables as local air temperature, wind movement, cloud cover, bridge location, orientation with respect to the sun, daytime solar radiation, and loss of heat by radiation into the night sky. Because of the poor thermal conductivity of concrete, diurnal temperature effects produce temperature gradients in a concrete bridge superstructure. The general heat equation which governs transient heat flow within the boundaries of the bridge superstructure is expressed as:

$$\frac{\partial T}{\partial t} = \frac{k}{\rho\, c} \frac{\partial^2 T}{\partial x^2},$$

where T = temperature of the bridge

t = time

x = direction in Cartesian co-ordinates

k = thermal conductivity

ρ = density

c = specific heat

In real life, a simple but reasonable solution can be obtained by assuming average values for the secondary parameters and assuming a sinusoidal effective temperature cycle. (One initial condition must be imposed in solving the previous equation. Since T is a temperature measured with respect to an arbitrary reference temperature, it is possible to choose this reference temperature as the uniform initial temperature of the bridge at t = 0. Then, the initial condition becomes T(x,o) = 0 and T(x,t) becomes the rise in temperature above its initial value).

At the upper surface of a bridge, conductive and convective heat transfer is controlled by the surface heat transfer coefficient, h. This is a function of variables such as the colour, texture and type of material used on the bridge surface, and the velocity of the wind blowing across the bridge surface. Given that the state of current research is such that only approximate values can be determined for bridge surfaces, the American Society of Heating, Refrigeration, and Air Conditioning Engineers (Hirst) suggests that for forced convection including average re-radiation

$$h = 1.3 + 0.62\ V^{3/4},$$

where V is the average wind velocity in miles per hour (if V = 7.2, h = 4.0).

At the surface of the bridge deck, conservation of heat flux at the surface boundary applies. Therefore, the net heat flux lost from conduction and convection into the surrounding air is equal to the normal component of the heat flux absorbed from the sun. The heat absorbed by the bridge deck from the sun is bI where b is the absorptivity of the surface to solar radiation. (Absorptivity is a dimensionless number between zero and unity). I is the normal component of both diffuse and direct shortwave heat flux from the sun (solar radiation in BTU per square foot hour or Watts/m^2hr). The conduction and convection heat loss is approximated by $h(T_E-T_A)$, where h is the surface coefficient in BTU per square foot hour degrees Fahrenheit. T_A is the air (shade) temperature (degrees Fahrenheit) and T_E is the effective temperature of the air (degrees Fahrenheit).

Equating the two relations, we obtain

$$h(T_E - T_A) = bI \text{ or } T_E = T_A + bI/h$$

Thus we have an expression for the effective air temperature including solar radiation.

The solar radiation which is received on a horizontal surface is either retained reflected, or re-radiated to the atmosphere. It is usually reported in langleys per day, L, which is 3.69 BTU per

square foot day. The average net loss by long IR wavelength re-radiation is 0.33 (Zuk), so that R, the average contribution to effective air temperature, is

$$R = \frac{0.67(b)\ 3.69(L)}{24h} \text{ (Barber)}$$

Combining this with the air temperature, which is approximated by a sine wave with amplitude equal to the daily range in temperature, gives a sinusoidal effective temperature (Figure 4). The mean effective air temperature is calculated from $T_M = T_A + R$ the maximum variation in the temperature from the mean, in degrees Fahrenheit, is $T_v = 0.5\ T_R + 3R$ where T_R is the daily range in air temperature. If the ambient air temperature varies as $T_M + T_v \sin \frac{2\pi t}{p}$, where in our case, p (the period) is 24 hours, we get from 16 for a steady state solution

$$T = T_M + \frac{T_v H \exp\left[\frac{-x}{l}\right] c}{\sqrt{(H^2 + c^2) + c^2}} \sin\left(0.262t + xc - \frac{\text{arctanc}}{H + C}\right)$$

where T is the temperature at the surface of the sound/delaminated deck
H, T_M, T_V have been previously defined in degrees F.

t = time from the beginning of a cycle in hours

x = is the depth of the delamination from the surface

H = h/k

h = surface coefficient BTU/ft^{2}hr°F

k = conductivity BTU/ft^2/hr[°F/ft]

$C = \frac{\sqrt{0.262}}{2(c)}$

c = k/sw diffusivity ft^{2}hr

s = specific heat BTU/lb°F

w = density lb/ft^3

The approximations used to describe instantaneous conditions from available meteorological records, smooth out short term changes in ambient conditions. In the case of a bridge with a long thermal response time, such short term changes are critical when the theoretical parameters are compared with measured instantaneous temperatures. If both theoretical and short term responses are compared in the context of a daily average, more favourable comparisons result. (The steady-state solution assumes that the cycle of temperatures have prevailed for a long time, a lag is to be

expected after a sudden change in T_M, which is to be expected if the shade temperature fluctuation in Figure 25 is observed). Thus, when T_M changes, the observed temperatures do not rise as much as calculated. When there is a sudden change in temperature, the theoretical lag for a large period (>12 hours) and small x is (from Carslaw and Jaeger)

$$\text{lag} = \frac{x + 0.25}{(\pi ct)^{1/2}}$$

The lag for the experimental data in this report may be up to 6°C. Larger deviations between theoretical and calculated temperatures are probably due to less radiation being received than the average because of clouds over the measurement sight. (Clouds were not necessarily present at the nearest radiation measurement station 3 km from the test site.) In addition, with a cyclic approximation to the heating cycle, longwave re-radiation is underestimated and consequently, actual temperatures will be higher than theoretical ones. Estimates of k, c, ρ etc., will also produce variation between theory and reality. As well, beginning the temperature cycle at dawn with a bridge temperature uniform through its thickness, means that the theoretical analysis will underestimate instantaneous daily temperatures. (The differential temperature between the top and bottom of a bridge is a function of heat input during the day and consequently, is independent of the initial starting condition.)

The theoretical equation is subject to further limitations. For example, it cannot be used to cover a 24 hour period-the reason being that the boundary conditions have not been solved for the complex changeover of radiation from dusk to dawn; neither will it take into account the shape of the cross-section of deck, unless approximated by semi-infinite slabs.

The environmental conditions which control the shape of the distribution of temperature through the depth of the deck of a bridge are more complex and difficult to define than those which give rise to extreme minimum and maximum effective bridge temperatures. Figure 5 shows that, for a concrete bridge, the temperatures in the top 0.5 m of the deck are controlled by solar radiation (Emerson). From a depth of 0.5 m to within approximately 0.3 m of the soffit, temperatures are controlled by the weather conditions of the previous one or two days. Within the bottom 0.3 m, bridge temperatures are controlled by shade temperature and heat reflected or re-radiated from the ground beneath the bridge.

5/ Experimental Results

An experimental program was initiated to take actual temperature measurements of sound and delaminated areas of a bridge deck and to compare these with a theoretical heat flow model estimator. Such a comparison, along with the preceding theoretical analysis, would help to establish constraints on the application of IR thermography to bridge structures.

5.1/ Measurement of Temperature

It was decided to use copper/constantan thermocouples for measuring the variation of vertical bridge deck temperature gradients with time. The copper/constantan thermocouple combination has the advantage of not being affected by the environment, be it polluted air, water, or concrete. For this type of thermocouple, the calibration of e.m.f. against temperature is not linear, but is automatically compensated for by the recording equipment. A further advantage is that the calibration of the thermocouples does not change with time and the recording equipment can be some distance from the thermocouples.

Thermocouples were made in the laboratory from 24 gauge copper/ constantan cable by wrapping the copper lead around the constantan and soldering the ends together. Use of the solder introduces a third material into the measuring device, but this does not affect the relative temperature differences of the thermocouples as long as all the temperature probes are produced in the same manner and no dry joints exist.

The spacing of the thermocouples through the cross-section of a bridge was important. To measure the temperature gradients accurately, the thermocouples were spaced closer where the largest gradient was expected to be, i.e., towards the top of the section. For example, in concrete bridges, experience has shown that within the top 25 mm of deck, thermocouples should be no more than 12.5 mm apart. Throughout the remainder of the depth, a spacing of 25 mm is adequate.

The method used for installing the thermocouples was to drill 12 mm holes in the deck surface to within 12.5 mm of the bottom. Thermocouples spaced at 0, 12.5 mm, 25 mm, 50 mm, 75 mm, 100 mm, and 125 mm (from the surface of the deck) were then inserted into these holes. The thermocouples were tied (with thin wire) into a bundle so that the distance between them remained constant. The bundles were then cast into the deck by pouring concrete (containing fine aggregate)

into the hole and vibrating the concrete in the hole with a metal rod. The concrete was then allowed to set for 48 hours.

In order to minimize any interference from reflective differences in the surface of the study section, the surface of the deck was coated with a cement/ water mixture. (Asphalt covered areas were painted with a "driveway sealer" compound.) The coating was then allowed to dry for 48 hours.

It was hoped that the above method of implanting thermocouples produced no air pockets around the thermocouple junction, because this would effect the measured temperature. The introduction of a different material into the deck did not alter the heat flow characteristics of the monitored areas since the diameter of the drilled hole was, in all cases, much smaller than the area of concern. Also, since IR equipment deals strictly with energy emitted from the surface of the bridge, as long as the thermocouple hole was well compacted, the surface heat flow characteristics would not be altered.

The above method of inserting thermocouples is not as accurate as precasting them into the bridge deck, however, this was not possible in this study. In addition, slight errors in measured temperatures are introduced due to the proximity of the thermocouples to reinforcing steel (the thermal conductivity of steel is twice that of concrete).

5.2/ Measurement of Sun and Shade Temperature

In order to measure shade temperature, a thermocouple was suspended beneath the deck. Subsequent analysis of the records showed that positioning the thermocouple under the deck was not entirely satisfactory. The reason for this is the thermocouple had to be placed close to the bridge in order to protect it from direct sunlight and was consequently affected by re-radiation of heat from the bridge. The end result was that the response of the thermocouple to variations in shade temperature was dampened.

The sun temperature was measured by suspending a thermocouple about a metre away from the side of the deck. Placement away from the deck minimized the error due to the convection of heat from the surface. Temperature profiles, presented in a future section, demonstrate the extreme variability of the in-sun temperature.

5.3/ Recording of Temperature

The outputs from the thermocouple circuits were recorded on a Fluke Model 2200B Data Logger which has an accuracy of $\pm 0.1°C$. The recorder was run with a ribbon tape printer interval of 6 minutes, providing 10 readings per hour.

The recorded data was then manually transferred from the tape printout to a personal computer for processing and plotting. The data logger was used primarily because it was readily available and has proven reliable over several years. It was also designed to eliminate the flow of current through the thermocouple leads and thus it was not necessary to compensate for long lead lengths. As well, it automatically compensated for the non-linear calibration of e.m.f. against temperature.

5.4/ Experimental Data

Temperature profiles (for July 23, 1986) for an exposed concrete deck are presented in Figures 6-17. The data demonstrate that early in the morning (Figure 6), the surface temperatures of the delaminated and sound concrete deck are the same. (Sunrise was at approximately 6:00 am and consequently, heating of the deck began at this time.) A residue of the previous days heating is apparent from the temperature differential which exists between the sound and delaminated deck areas at depths greater than 25 mm. By 7:52 am, the surface thermocouples show a temperature difference. The sound deck area is cooler on the surface than is the delaminated deck area. Thus, the delamination is acting as an insulator. However, the area underneath the delamination is cooler than the area under the sound deck. It seems that because the delamination affects heat transfer, the solid deck is able to transfer heat to lower areas much more efficiently. The surface temperature differential continues to increase until it reaches a maximum between 11:00 am and 12:00 noon (Figures 10 and 11, respectively). At this time the temperature profiles below 12.5 mm begin to merge (their difference is decreasing). Subsequent to this, the surface temperatures begin to converge, while the temperatures at greater depths begin to diverge. Had the temperature monitoring continued for an entire day, a sinusoidally oscillating 24 hour variation would have been observed. The relative temperatures of the deck at its surface and at its interior, demonstrate that there is a time lag associated with solar heating. Consequently, the profiles in Figures 5 to 17 are not instantaneous temperatures related to time of solar heating. Rather, they are related to the solar heating and ambient weather conditions which were encountered at an earlier time in the day. In principle, this is based on the poor thermal conductivity of concrete. Only the surface temperature is directly related to the solar radiation of the last few minutes.

The above observations are consistent with previously published reports (Manning). However, there is one significant difference in that under delaminated concrete, the bridge deck is cooler than under the sound areas with lower surface temperature. To the authors knowledge, this information has never previously been acknowledged.

5.5/ IR Observations

While the temperature profile measurements were being collected, the energy emitted from the surface of the slab was being monitored using an Aga 720 infrared system. The scanner has the capability of measuring temperatures in the -50°C to 1500°C range when calibrated with an ultimate resolution of 0.1°C. The scanner uses an indium antimonide detector cooled by liquid nitrogen. A 20° lens was used, allowing the operator to view one full lane width with the scanner mounted 5 metres above the ground.

A schematic presentation of a section of exposed concrete bridge deck containing both sound and delaminated areas is shown in Figure 19. Figures 19 through 24 detail the changes of emitted energy during the course of the day.

At 6:52 am the IR scanner was unable to detect any difference between sound and delaminated areas of the bridge deck. However, by 7:30 am a hot spot had developed in the middle of the delaminated area. (The delaminated area was previously defined by careful sounding with a hammer. Subsequent drilling during insertion of the thermocouples showed that this delamination was at a depth of approximately 12 mm.) By 8:52 am a faint outline of the delaminated area was visible with the hottest spot occurring in the middle of the delamination. (The delamination outline was visible through careful gain adjustment of the IR scanner and would not be visible during the course of a normal deck survey.) At 9:52 am the delamination was readily visible through the IR scanner without any further gain adjustment.

From the IR imaging, it became obvious that heat was diffusing radially from the centre of the hot spot. Consequently, the shape of the delamination was becoming circular with the rough edges of the delamination smoothened out (see Figure 16). It appears that under direct solar radiation the time at which the IR "hot spots" are closest in area to the actual delaminations is between 10:00 am and 11:00 am. After this time, the radially diffusing hot spots overestimate the size of the delaminations relative to the rest of the bridge deck (see Figures 22, 23, 24).

By 5:00 pm the bridge deck had been sufficiently heated and there were no detectable temperature differences between the sound and delaminated areas. The deck surface appeared homogeneous through the IR scanner. Monitoring was discontinued after 6:00 pm.

At this point a note should be made regarding the importance of the IR scanner gain controls in relation to the observed hot spot(s).

In the above example, at approximately 9:00 am a hot spot, which is related to deck deterioration, appears on the bridge deck . With time, the hot spot appears to grow radially outward in intensity until a time (between 10:00 and 11:00 am) when it becomes an excellent representation of the delamination. The job of the operator is to optimize the equipment gain and IR resolution so that the deterioration is detectable. However, with time, the intensity of solar radiation increases, as does the energy reflected and emitted by the bridge deck (due to its absorptivity). Consequently, the morning IR scanner gain settings become inadequate later in the day. This is caused by the rise in reflected and emitted energy which overloads the amplifier in the IR system. To compensate for this, the gain control must be adjusted. Constant resetting of the gain eliminates the ability to make comparisons between two areas of a bridge deck. The reasons for this is as follows:

1) The different IR energy levels emitted from the bridge deck are detected by the Aga scanner.

2) The scanner converts the absorbed energy into an electronic signal which is subsequently converted into a picture element (grey scale) on a video monitor. When the gain is changed on the IR controller, the grey scale pixel level also changes. Consequently, if two adjacent thermograms are compared (and the comparison is based solely on the pixel grey level), the gain adjustment must remain the same for both thermograms. Otherwise, the grey level in one thermogram will have no relation to that of any other thermogram.

As a result, when performing surveys on multiple lane bridges, it is critical that all the lanes be scanned in as short a time as possible. Otherwise, gain adjustments will be necessary and it will not be possible to compare IR thermograms from different scans.

5.6/ Thermocouple Data From Asphalt Covered Decks

Thermocouples were embedded into an asphalt covered bridge deck in the same manner described in the previous section. The only difference was that cold mix was used for the upper thickness of "fill" between the thermocouples rather than concrete. As before, the lower concrete component

was filled with concrete consisting of a fine aggregate. The surface of the asphalt was then coated with a "driveway sealer" to provide a similar absorption coefficient for both the delaminated and sound areas of the bridge deck.

The thermocouples used were 24 gauge copper/constantan. As in the exposed concrete deck measurements, the thermocouples were spaced at 0, 12.5 mm, 25 mm, 50 mm, 75 mm, 100 mm, and 125 mm (from the surface). The thermocouple readings were accurate to $\pm$0.1°C.

The results of the thermocouple survey are shown in Figure 25. Erratic variation of temperature with time is evident from this figure. In particular, there is a significant high frequency temperature variation on the asphalt surface overlying the delamination. The variation of surface temperature with time is not as severe at the surface of the asphalt overlying solid deck. (The data was collected on July 30, 1986 on the Winston Churchill overpass over Highway 401. It was a day of high intensity solar radiation with no discernible cloud cover and a maximum monitored wind velocity of 10 km/h). A low frequency daily temperature variation is also apparent from the diagram. The plot shows that the surface temperature over delaminated deck is much more susceptible to instantaneous solar radiation changes than over solid bridge deck. (The instantaneous change is critical to IR surveys because gain adjustment to the IR equipment may be required in order to maintain proper temperature resolution. As previously discussed, this is not desirable for data processing.) Consequently, it is imperative to perform all IR scans of a bridge deck in as short a time as possible in order to minimize the effects and difficulties of the high frequency temperature components.

A detectable temperature difference between sound and deteriorated deck does not appear until after 8:00 am. With an average of 65 mm of asphalt overlay, a maximum temperature differential occurs between 12:00 noon and 1:00 pm. This was found to be a common time range for maximum IR resolution on asphalt covered decks with less than 75 mm of asphalt. The asphalt overlay was found to shift the time at which the optimum temperature differential occurs by 1 to 2 hours. Later in the day, the plot demonstrates that the surface of the asphalt covered delamination takes approximately an hour longer than the exposed concrete deck to cool below the temperature of the surrounding sound bridge deck. These results suggest that the insulation value of the asphalt surfacing compensates for the greater heat absorption associated with the darker surface.

The one sharp dip in temperature in Figure 25 (at approximately 12:30 pm) is most likely due to a glitch in the data logger. The temperature at this time is not consistent with the temperatures preceding and following the dip. In addition, it is impossible to visualize such a large temperature

change in such a short period of time, with no apparent change in the ambient environmental condition.

The Winston Churchill Bridge deck was also monitored between 12:00 noon and 1:00 pm using the infrared system. Once the IR camera and van were in position, a reference point was selected and the distance measuring device was zeroed. The pavement was then scanned. During the scanning operation the van was stopped periodically at areas showing deterioration for the purpose of ground truthing the infrared data. The pavement was then marked and surface temperatures measured with a contact thermometer to confirm a surface temperature difference between the delaminated and adjacent non-delaminated areas. After temperature measurement and pavement marking, the remainder of the pavement was scanned. Five areas marked as "hot spots" were subsequently cored. Three of the five cores taken showed evidence of delamination. One area, which was thought to be delaminated, showed evidence of scaling. The fifth hot spot had a surface temperature difference of 4.3°C between it and the adjacent "cooler" deck. However, coring provided no evidence of delamination. As there was no apparent difference in surface absorptivity to cause the difference in observed temperature, it is thought that the asphalt may have been debonded. Visual evidence in the core hole itself was inconclusive.

6/ Summary

1) This study has shown that infrared thermography, obtained from a ground based vehicle mounted platform, is an effective method for detecting and mapping deterioration in exposed concrete and concrete or asphalt overlay bridge decks.

2) The infrared system of deterioration detection is effective when applied to one lane approximately 4 m wide. By using a continuous method of scanning, recording, and play back, any length of bridge deck can be accommodated. Surveys in this report were conducted on a lane by lane basis at a maximum speed of 4 km/h. Faster survey speeds were found to distort the digitized version of the infrared image.

3) The sensitivity of the IR system has been demonstrated in previous thermographic camera studies (Manning and Holt). The reliability however, would be greatly improved if the actual deck surface was recorded simultaneously with the IR.

4) From experience and literature, it is known that IR systems do not operate if the deck surface is covered with rain, snow, or standing water.

   Precipitation preceding the survey day must be taken into account. If water has accumulated in a delaminated area, it will act as a continuum heat sink for impinging solar radiation. Since water has a large latent heat of vaporization, most of the surface heat will be absorbed and transferred by the water. As a result, deterioration will not be detected by the IR system. Two IR surveys performed on the Winston Churchill overpass confirmed this idea. On a hot day (32°C) with no wind, high irradiance, and no previous rain (six days), several delaminations were visible on the bridge deck. Three weeks later, on a cooler day (18°C) with no wind and high solar irradiance, several of the previously visible delaminations were not detectable using the IR system, even though theoretically the weather conditions were more favourable. Upon closer examination, it was discovered that there was water underneath the asphalt surface, a consequence of rain the previous three days. As a result, it was determined that not only must the weather conditions be noted on the day of the survey, but also, consideration should be given to precipitation on days prior to the survey.

5) Operation of the IR system should be limited to clear sunshine (or at most 10% cloud cover). Observed temperature differentials can reach 9°C on a very sunny day on asphalt covered

bridge decks or 5°C on exposed concrete decks. If clouds are present, the temperature differential between deteriorated and sound surfaces will not be as great and therefore will be more difficult to detect. The complete effect of cloud cover on bridge deck heating is unknown, but the IR signals will be reduced due to the reduction in solar radiation. In addition, the reflected and emitted IR spectrum must remain constant in subsequent IR processing and mapping. If the solar irradiance is changing randomly, the recorded grey scale infrared images will change accordingly (fading in and out). This makes comparisons of different parts of a bridge deck difficult, as it is impossible to set a certain colour pixel to represent the deteriorated area.

6) Previous studies (Goldstein) have indicated that high winds effectively neutralize bridge deck temperature differences, but that light winds probably have little effect. While wind velocity is an important component in theoretical calculations of bridge deck temperature differences, wind velocity was not a determining factor during field trials. On several exposed concrete and asphalt covered bridge decks, winds gusting up to a maximum of 60 km/h under clear skies were observed. However, the relative temperature differences observed through the IR system did not change because of the gusting. In addition, when steady winds up to 50 km/h were blowing during a survey of the MacDonald-Cartier Bridge in Ottawa (asphalt covered), deterioration was readily visible through infrared imaging. From these observations, it is concluded that under clear sky conditions, wind velocities of up to 50 km/h will not affect IR surveys.

7) The best time for IR operation (in Southern Ontario) is from 10:00 am to 11:00 am on exposed concrete and from 12:00 noon to 1:00 pm on asphalt covered bridge decks. At these times, the temperature differences between unsound and sound bridge deck areas are most easily distinguished. More importantly, the area of the hot spots best approximates the actual size of the deteriorated areas. Temperature differentials were found to exist at almost any time of the day except around sunrise and sunset. After sunrise, when the deck begins to warm, the surface temperature of the deteriorated region changes from being cooler to hotter than the average deck surface temperature. The reverse situation occurs shortly after sunset.

8) For asphalt covered bridge decks with less than 75 mm of asphalt, the best time for delamination detection is between 12:00 pm and 1:00 pm. It is essential that asphalt covered decks receive a reasonably constant amount of solar radiation before measurements are made. After 3:00 pm the deck begins to cool due to reduced solar radiation. Under such conditions,

the contrast between a sound and unsound deck is reduced and sometime before sunset the temperature differentials become undetectable.

Scaling of the concrete below the asphalt is a fairly unique thermal image in that it appears as a mottled grey-white tone. The more severe and extensive the scaling, the more mottled the thermal image appears.

The IR scanner does not easily allow the operator to identify debonding. The debonding, at times, appears to be hotter than adjacent delaminations. Depending on the thickness of the delaminations, the debonding can appear identical to delaminations or even invisible to IR thermography.

9) If surveys are carried out at the times noted above, then a temperature differential of 1.5°C to 2°C is a reasonable practical minimum to counteract the effects of differences in emissivity caused by such factors as polishing wheel tracks, staining, and patching.

10) As a rule, when there is more than 75 mm of asphalt on top of a delamination, not enough of a temperature differential will be generated by solar heating to be resolvable by IR. In some instances, scaling and debonding will be seen with up to about 75 mm of asphalt overlay. If more than this amount of asphalt exists, rarely will deterioration be detected. Thermocouple measurements have shown that the temperature at the asphalt surface varies linearly with the thickness of bituminous surfacing up to 50 mm.

11) The properties of the wearing course affected both the amount of heat energy absorbed at the top face of the bridge and its transmission downward.

Asphalt has a higher absorptivity than a normal grey-white concrete deck, and the surface temperature of a deck with asphalt will be different from that of a concrete deck under identical climatic conditions. The amount of radiant heat energy absorbed is a function of the absorptivity to solar radiation of the top surface. This can vary from 0.96 for freshly laid asphalt to 0.50 for concrete or asphalt subject to traffic. Absorptivity will also vary when the surface is washed by rain. Consequently, comparing thermographs from different days is difficult. As solar radiation is the dominant heat transfer mechanism affecting temperature differentials, any action which changes the value of absorptivity will have a direct impact on the IR imaging.

12) The time of year for optimum testing will depend upon the climate. In Toronto, the maximum temperature differentials occur in early or late summer. Ambient temperatures in the range of -32°C to 32°C were investigated and were not found to have a significant effect on the detectability of deterioration. Differentials were greater in the summer than in the winter because of the increased intensity of solar radiation. The major effect of the ambient temperature was to lengthen or shorten the scanning "window" time.

13) Normal traffic density did not seriously affect the infrared inspection technique. If the traffic density was such that it materially lowered the solar irradiance, temperature differences were affected. Such a condition existed where a number of vehicles cast shadows on the roadway for an extended period of time. Stalled traffic would also restrict solar radiation, eliminating the possibility of a survey under such conditions. Some heating effects have also been observed from the engines of slow moving vehicles, however, at highway speeds this would not be a problem.

14) Traffic on adjacent lanes will not influence the results. Transient shadows of large vehicles have been observed. However, these move rapidly enough not to affect the IR image.

15) Densely packed sand and gravel on the surface will affect IR surveys. If this condition exists, the bridge deck should be swept the day before the actual survey.

16) The use of an infrared camera with a short wavelength IR capability (2 to 5.6 microns) proved to be superior to a longer wavelength (6 to 12 microns) camera. There are several reasons for this:
    a) At the longer wavelengths, IR cameras are more sensitive to IR energy emitted from secondary objects (guardrails, signs, fixtures, etc.). Consequently, the resolution in the higher wavelengths is reduced because of the additional effect of the extraneously emitted thermal energy.
    b) The higher wavelength equipment is also more sensitive to internal camera "noise". That is, in tests, the shorter wavelength equipment inherently had a lower signal to noise ratio than did the 6 to 12 micron wavelength equipment. This provided the 3 to 5.6 micron wavelength range with more resolution that the longer wavelength detectors.

17) A correlation existed between temperature differential and thickness of the delaminated concrete. In general, the temperature difference was larger for more serious delaminations. The surface temperature was influenced by the depth of the defect because there was a loss in

IR resolution as the depth of the defect increased. Consequently, resolution was enhanced for defects near the surface.

18) The orientation of defects cannot be determined since one observes only a surface temperature difference not the actual effect below the surface. The orientation of the defects, however, will certainly have an influence on the surface temperature.

19) Theory: The foregoing theory indicates the possibility of roughly correlating theoretical surface temperatures with actual measured values, so that a means is available to extrapolate field observed temperatures to other times and places. To calculate the exact temperature for a given structure place and time, exact values of its thermal properties and ambient condition must be known.

The experiments and analysis examining the application of infrared thermography to bridge deterioration are in agreement. They both bring forth quite clearly the difficulties encountered in quantitative determinations of solar induced emission of heat energy. The analysis shows the sensitivity of the surface temperature to surface emissivity, sky radiation, and wind speed. This is verified experimently since concrete decks have very different characteristics than asphalt covered ones. On decks with a relatively high emissivity in the infrared, the theoretical derivation can provide reasonable approximations to relative surface temperatures. However, care must be taken when using the theoretical equations because significant real microclimate temperature variations may occur across the field of measurement of the scanner. Structures in very close proximity to weather stations might be expected to have similar microclimates — primarily wind speed and air temperature. However, since all the parameters required for the theoretical temperature calculations are often only estimates or daily averages, comparison of theoretical temperatures with actual deck temperatures at any instant in time is very difficult. (This is verified by observing the extreme variation of surface temperatures presented in the experimental section of this report. The same extreme variation does not occur below the surface of the monitored decks.) Measurement of surface temperature is not the usual goal of infrared thermography. Rather it is a stepping stone enroute to detecting temperature differentials which exist in deteriorated bridge decks. Theoretical results show that a change in b (absorptivity) from 0.6 to 0.7 may produce a temperature drop change of 1.0°C (all other factors remaining constant). The trend in temperature is clearly in the expected direction, but the scatter is usually so large as to preclude any quantitative judgements other than in very special situations. In reality, the surface of a bridge deck is not homogeneous and any variation due to b (more notably due to rain washing of the deck surface rather than oil spots,

patching, skid marks, etc., which are easily recognizable) results in noticeable changes in IR emissivity. This may lead to areas of deterioration being missed by the IR cameras.

Perhaps the most influential of the parameters considered in the theoretical temperature calculations is the wind speed. With all factors remaining equal, a doubling of wind speed from 10 km/h to 20 km/h effectively changes the surface temperature (downward) by 0.5°C. Therefore, wind speed in theory should be critical to IR surveys. In practice however, wind speed did not appear to affect the capabilities of the IR equipment. (This may in part be due to the method used for measuring wind speeds. The wind speed was always measured above obstructions (guardrails, etc.). The wind which effects IR emissivity is at surface level. Consequently, the wind speed at ground level was not necessarily the same as above the guardrail, possibly accounting for the observed discrepancy of wind effect between theory and practice.)

The assumption that all temperatures through the deck are uniform and equal to some temperature at sunrise is seen to give rise to the largest error in the calculated gradients during the first few hours of the calculation. This error however, is reduced as the calculations progress.

What is seen from the preceding results is that the IR system does locate and display to a usable scale, deterioration in bridge decks. The existence of temperature differentials and gradients have experimentally been shown to exist consistent with theoretical predictions. The most critical parameters for the generation of observable temperature differentials were observed to be solar irradiance and emissivity. However, as wind speed is critical to the theoretical calculation of emissivity, it is important that wind speed at the surface of the bridge deck be carefully monitored when performing IR surveys.

7/ Comments and Recommendations

This research has demonstrated that thermography is an effective tool for detecting and mapping delaminations in reinforced concrete bridge decks under clear sky conditions.

The black/white hardcopy printing mode used for printing the thermographic images, does not allow for the filtering out of unwanted responses. It is therefore recommended that a grey-scale plotting system be acquired for hardcopy output.

Since hardcopy output is a grey-scale interpretation of a thermographic image, solar irradiance must not change during the course of a scan of a bridge deck. Otherwise, colour levels from one section of the bridge deck will have no correlation with other parts of the bridge deck in the hardcopy output. Therefore, clear sky conditions are recommended for IR surveys. However, some cloud cover is acceptable, but only if the clouds do not mask more than 10% of the solar radiation during an IR scan. If this occurs during a pass, the IR image will become dark (or black) on the monitor requiring the lane scan to be repeated.

While wind has an important effect (in theory) on the emitted IR energy from the bridge deck, wind speeds up to 60 km/h did not appear (in practice) to affect IR scans. Published reports have indicated that if wind was affecting the IR image, the image would fade in and out (flicker) on the IR monitor. This phenomena was never observed by the author, but should be watched for.

Finally, the previous day's precipitation should be monitored prior to doing an IR survey because moisture in deteriorated areas will act as a heat sink, severely attenuating emitted IR energy.

8/ References

1. Alford, J., Ryan, J., and Urban, O., "Effect of Heat Storage and Variation in Outdoor Temperature and Solar Intensity on Heat Transfer Through Walls", American Society of Heating and Ventilation Engineers, Vol. 45, 1939.

2. Barber, E.S., "Calculation of Maximum Pavement Temperature from Weather Reports", HRB Bulletin 168, 1957.

3. Carrier, G., and Pearson, C., "Partial Differential Equations", Academic Press, 1976.

4. Carslaw, H.S., and Jaeger, J.C., "Conduction of Heat in Solids", Oxford Press, Vol. 2, 1949.

5. Shen, C.H., and Krokosky, E.M., "Steady and Non-Steady Solar Heat Transmission Through Roofs", ASHVE Trans., Vol. 71, 1972.

6. Emerson, M., "The Calculation and Distribution of Temperature in Bridges", TRRL Report LR561, 1973.

7. Emerson, M., "Bridge Temperatures", TRRL Supplementary Report 442, 1977.

8. Gloyne, R.W., "The Diurnal Variation of Global Radiation on a Horizontal Surface", Meteorological Magazine 101, February, 1972.

9. Goldstein, R.J., "Quantitative Thermography - Estimation of Building Envelope Heat Losses", University of Minnesota, Internal Report 3/5-A, October, 1982.

10. Hafermann, G., "Application of Thermal Imagery on CR CP and Bridge Decks", Final Report, Wisconsin Department of Transportation, FHWA/WI-83/1, July, 1983.

11. Hirst, M., "Solar Heating of Bridges", Australian Road Research, Vol. 11, No. 2, June, 1981.

12. Hunt, B., and Cooke, N., "Thermal Calculations for Bridge Design", Proc. American Society of Civil Engineering, J. Structural Division 101 (5T9), September, 1975.

13. Imbsen, R.A., Vandershaf, D.E., Schamber, R.A., and Nutt, R.V., "Thermal Effects in Concrete Bridge Superstructures", TRB NCHRP Report 276, September, 1985.

14. Jones, M.R., "Bridge Temperatures Calculated by a Computer Program", TRRL Report 702, 1976.

15. Kehlbeck, F., "Effect of Solar Radiation on Bridge Structures", Dusseldorf Werner-Verlag, 1975.

16. Kunz, J., "Infrared a Hot Technology", Consulting Engineers, September, 1986.

17. Manning, D.G., and Holt, F.B., "The Development of DART", Ontario Ministry of Transportation and Communications, Report ME-85-03, 1985.

18. Mortlock, J.D., "The Instrumentation of Bridges for the Measurement of Temperature and Movement", TRRL Report 641, 1974.

19. Prakash Rao, D.S., "Temperature Distribution and Stresses in Concrete Bridges", ACI Journal No. 83-52, July, 1986.

20. Priestly, M.J., "Effects of Transverse Temperature Gradients on Bridges", Ministry of Works, New Zealand, Report #394, September, 1971.

21. Radolli, M., and Green, R., "Thermal Stresses in Concrete Bridge Superstructures Under Summer Conditions", TRRL No. 547, 1975.

22. Rossiter, W., and Clifton, R., "The Use of Non-Destructive Methods for Inspecting Single-Ply Roofing Membranes", Durability of Building Materials 3, 1986.

23. Sears, F., and Salinger, G., "Thermodynamics, Kinetic Theory and Statistical Thermodynamics", Addison-Wesley Publishing, 3rd Edition, 1975.

24. Tsutsumi, S., and Takemura, K., "Sensing Technique to Identify and Locate Surface Defects on Highways", Symposium on Noise and Clutter Rejection in Radars and Imaging Sensors, Japan, 1981.

25. White, I.G., "Non-Linear Differential Temperature Distributions in Concrete Bridge Structures", Cement Conc. Assoc., Technical Report 525, 1979.

26. Zuk, W., "Thermal Behaviour of Composite Bridges - Insulated and Uninsulated", Highway Research Record 76, 1965.

Type of Aggregate	Density of Concrete kg/m^3	lb/ft^3	Conductivity $J/m^2s\ °C/m$	$Btu/ft^2\ °F/ft$
Barytes	3640	227	1.38	0.8
Igneous	2540	159	1.44	0.83
Dolomite	2560	160	3.68	2.13
Lightweight Concrete (oven-dried)	480-1760	30-110	0.14-0.60	0.08-0.35

Table 1/ Typical Values of Thermal Conductivity of Concrete

Unit weight		Conductivity J/m^{2}s °C/m Btu/ft^2 °F/ft						
		For concrete protected from weather			For concrete exposed to weather			
kg/m^3	lb/ft^3	Aerated concrete	Lightweight concrete with foamed slag	Lightweight concrete with expanded clay or sintered fly ash	Normal weight aggregate concrete	Aerated concrete	Lightweight concrete with foamed slag	Lightweight concrete with expanded clay or sintered fly ash	Normal weight aggregate concrete
320	(20)	0.109 (0.063)	0.087 (0.063)	0.130 (0.075)		0.123 (0.071)	0.100 (0.058)	0.145 (0.084)	
480	(30)	0.145 (0.084)	0.116 (0.067)	0.173 (0.100)		0.166 (0.096)	0.130 (0.075)	0.187 (0.108)	
640	(40)	0.203 (0.117)	0.159 (0.092)	0.230 (0.133)		0.223 (0.129)	0.173 (0.100)	0.260 (0.150)	
800	(50)	0.260 (0.150)	0.203 (0.117)	0.303 (0.175)		0.273 (0.158)	0.230 (0.133)	0.332 (0.192)	
960	(60)	0.315 (0.182)	0.260 (0.150)	0.376 (0.217)		0.360 (0.208)	0.289 (0.167)	0.433 (0.300)	
1120	(70)	0.389 (0.225)	0.315 (0.182)	0.462 (0.267)		0.433 (0.250)	0.360 (0.208)	0.519 (0.300)	
1280	(80)	0.476 (0.275)	0.389 (0.225)	0.562 (0.325)		0.533 (0.308)	0.433 (0.250)	0.635 (0.367)	
1440	(90)		0.462 (0.267)	0.678 (0.392)					
1600	(100)		0.549 (0.317)	0.794 (0.459)	0.706 (0.408)				0.808 (0.467)
1760	(110)		0.649 (0.375)	0.952 (0.550)	0.838 (0.484)				0.952 (0.550)
1920	(120)				1.056 (0.610)				1.194 (0.690)
2080	(130)				1.315 (0.760)				1.488 (0.860)
2240	(140)				1.696 (0.980)				1.904 (1.100)
2400	(150)				2.267 (1.310)				2.561 (1.480)

Table 2/ Values of Conductivity

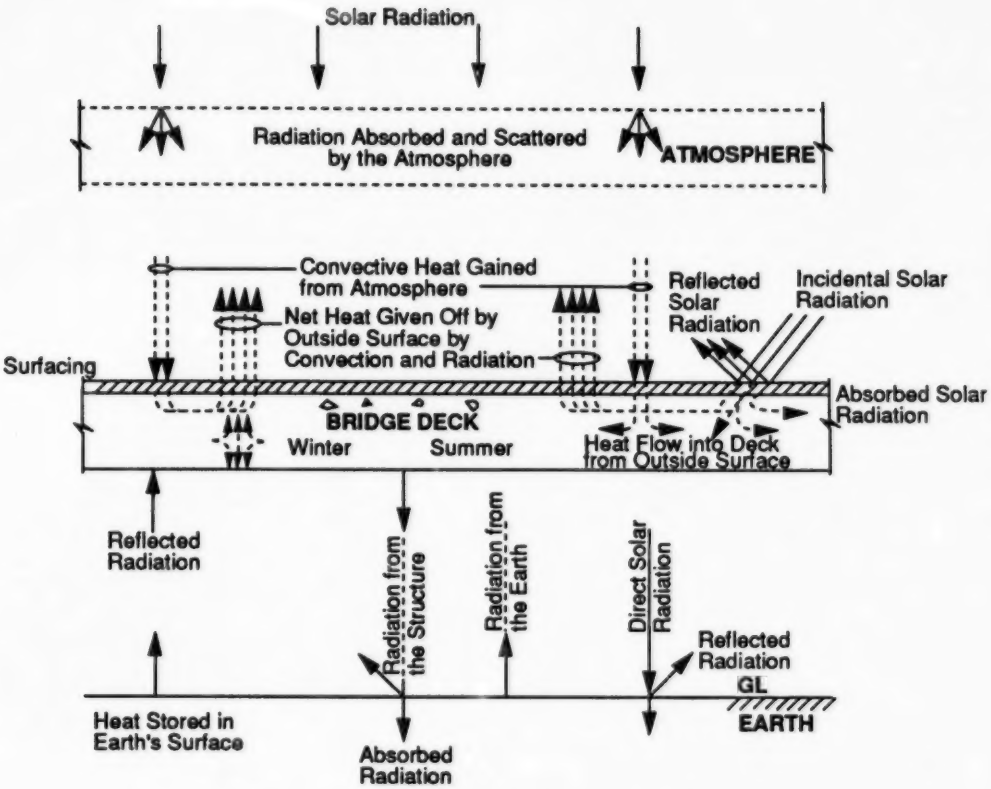

Figure 1/ Solar Radiation Reaching the Surface of a Bridge

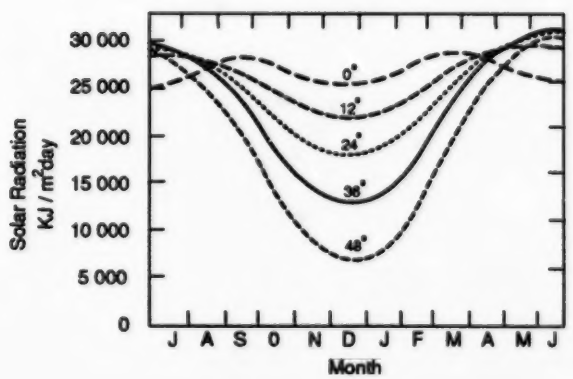

Figure 2/ Variation in Solar Radiation for Various Latitudes

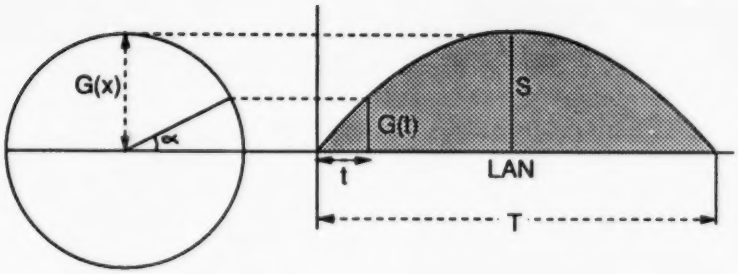

Figure 3/ Co-ordinate System for Estimation of Diurnal Course of Global Radiation on a Horizontal Surface

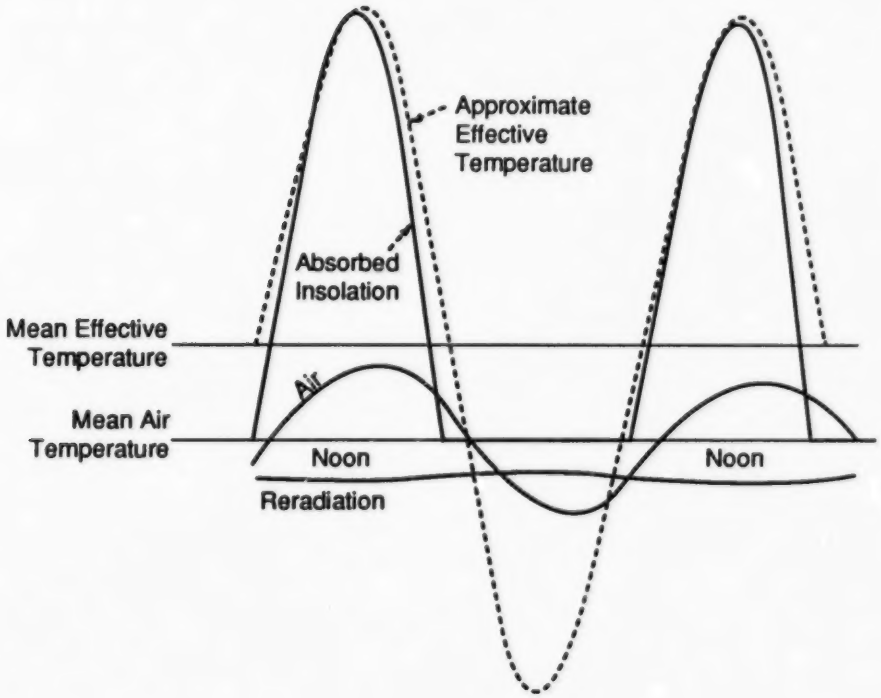

Figure 4/ Effective Temperature Above Horizontal Surface

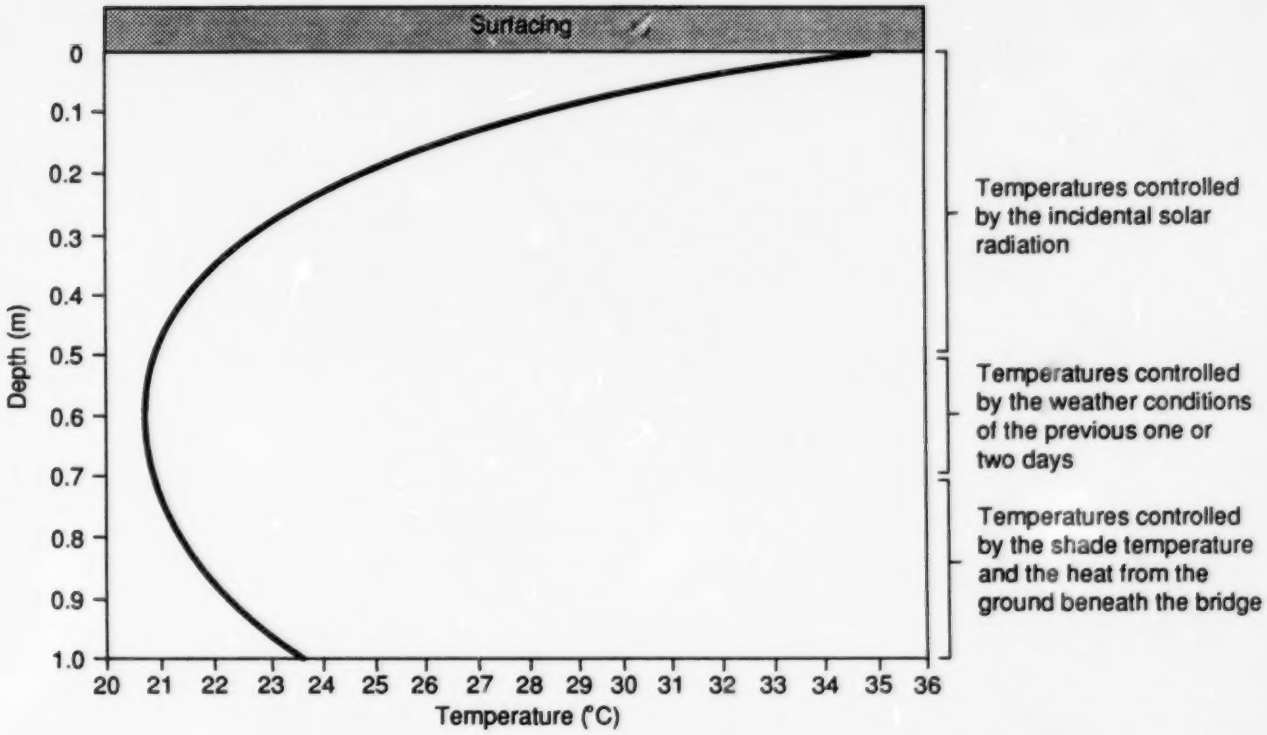

Figure 5/ The Environmental Conditions Which Control the Shape of a Temperature Distribution

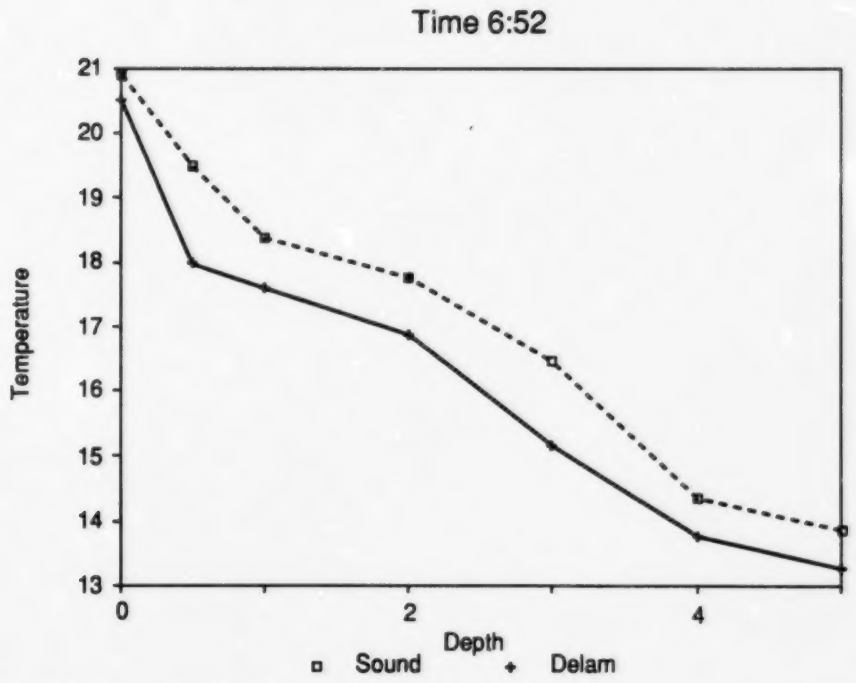

Figure 6/ Infrared Image at 6:52

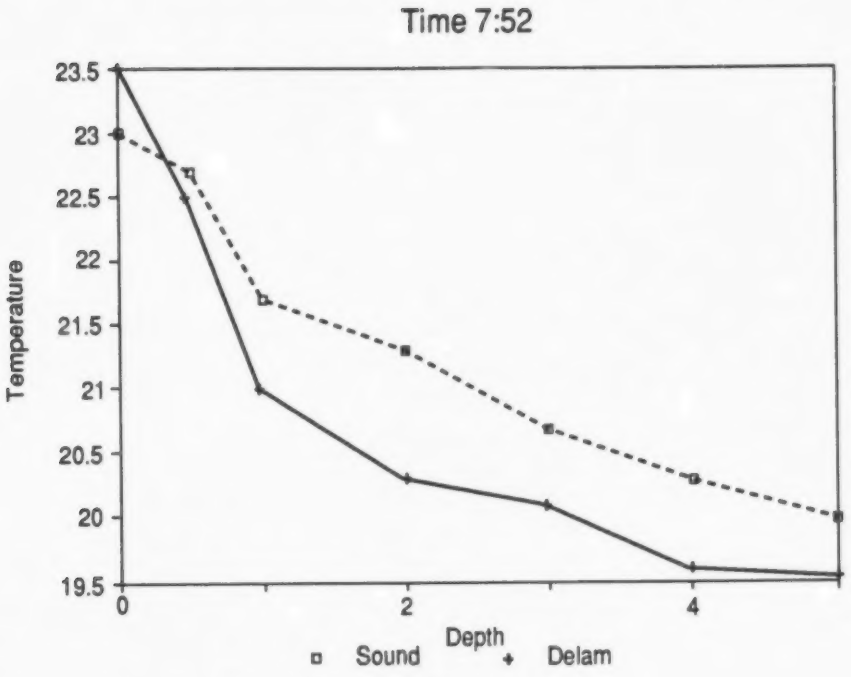

Figure 7/ Infrared image at 7:52

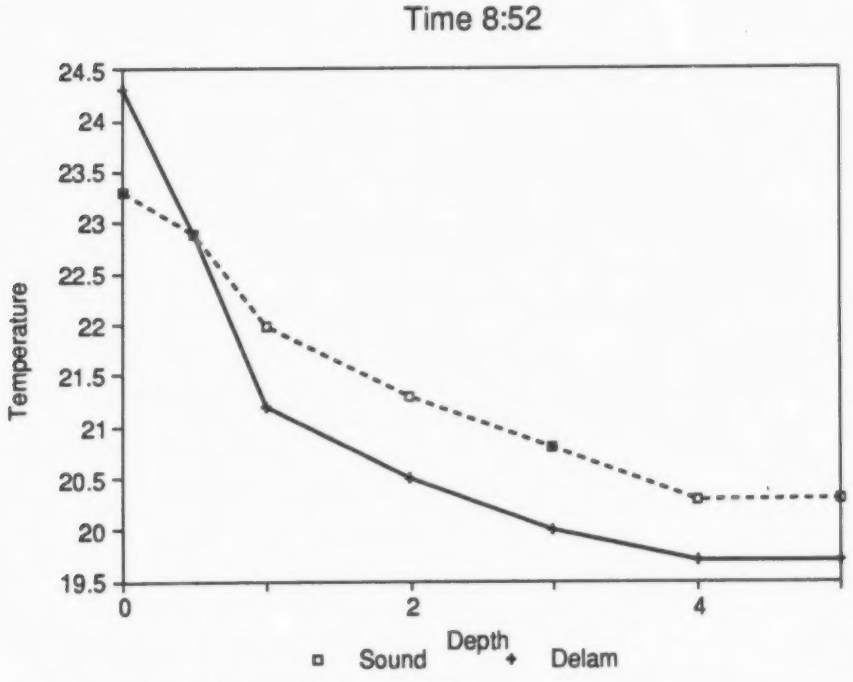

Figure 8/ Infrared image at 8:52

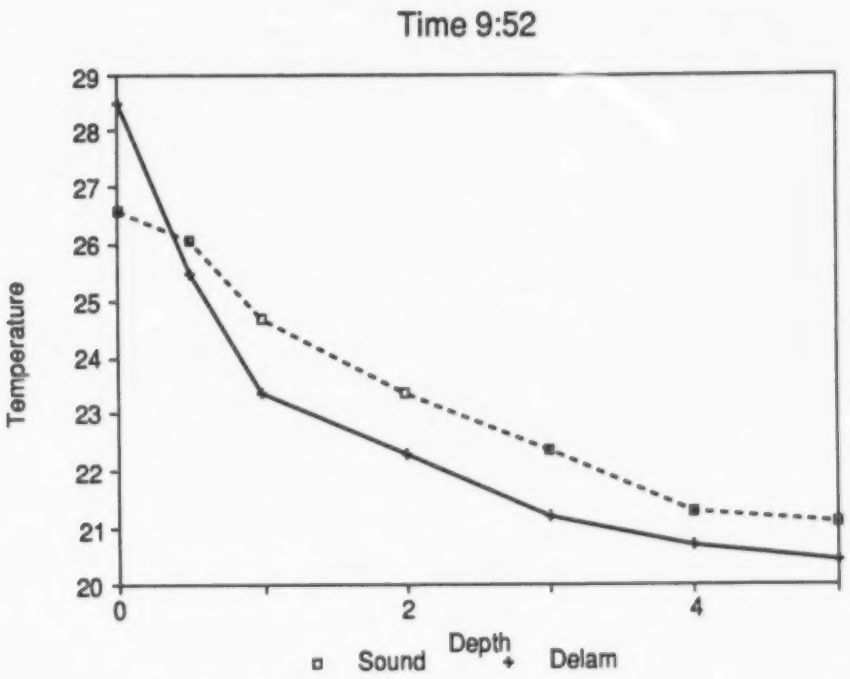

Figure 9/ Infrared Image at 9:52

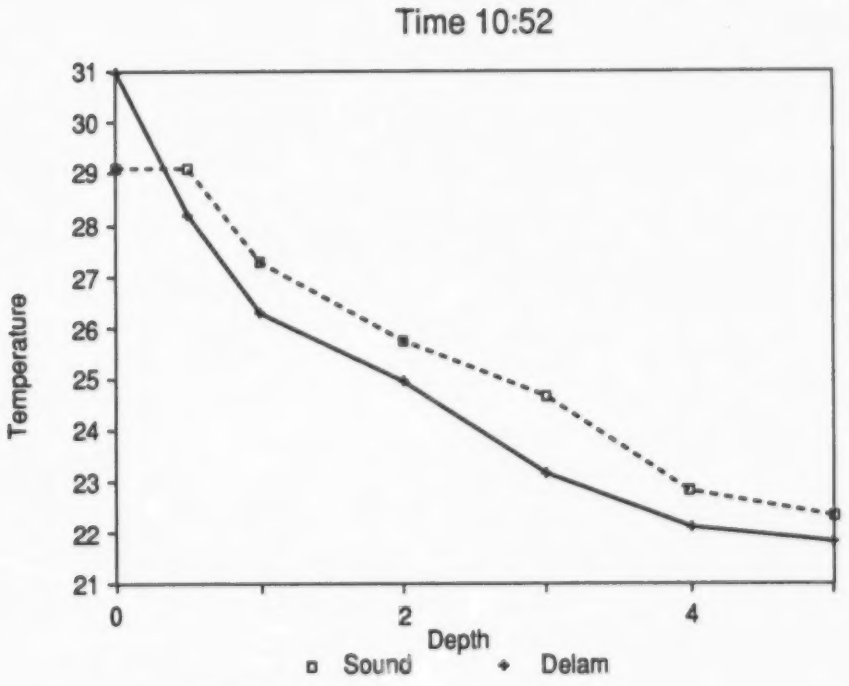

Figure 10/ Infrared Image at 10:52

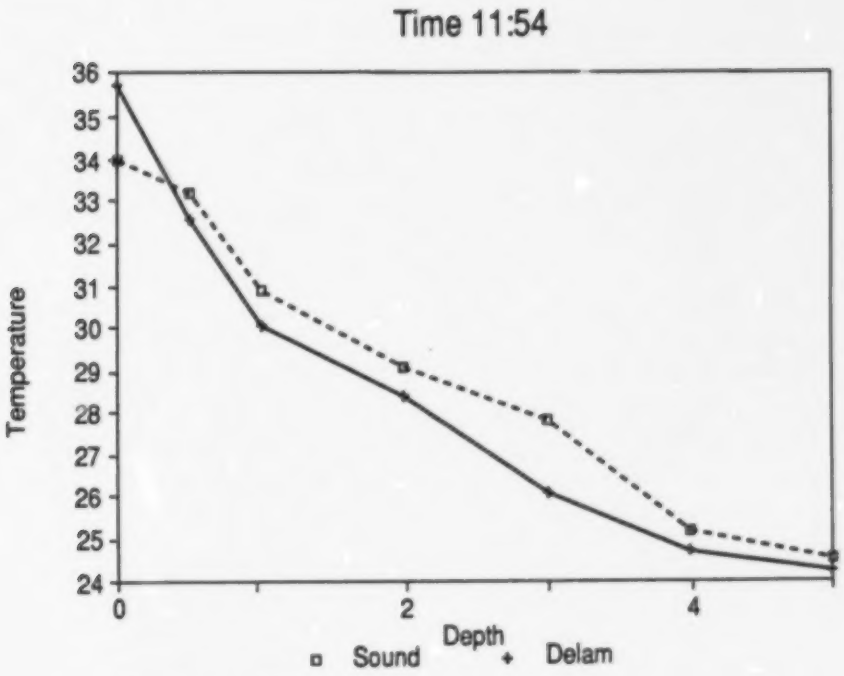

Figure 11/ Infrared Image at 11:54

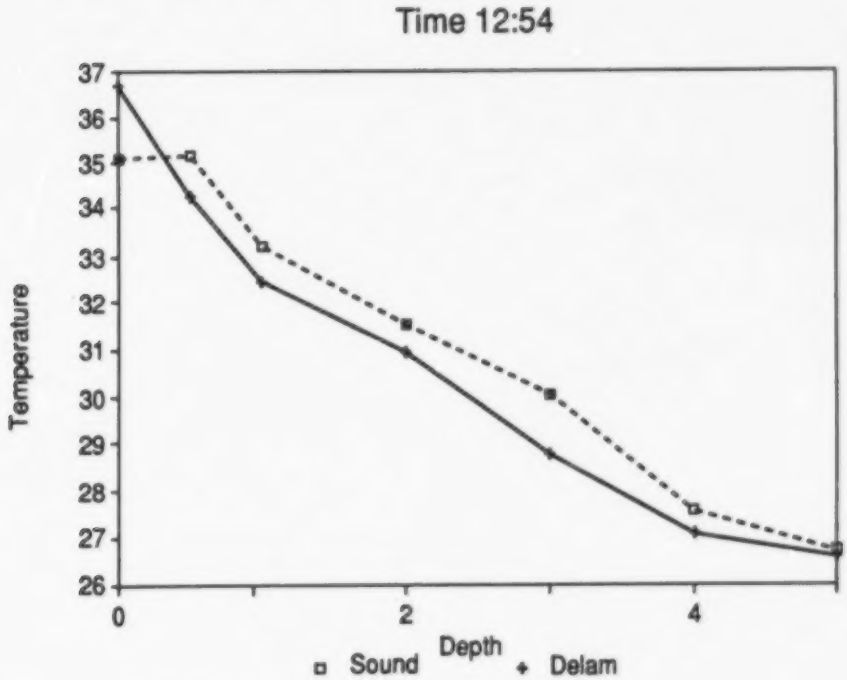

Figure 12/ Infrared Image at 12:54

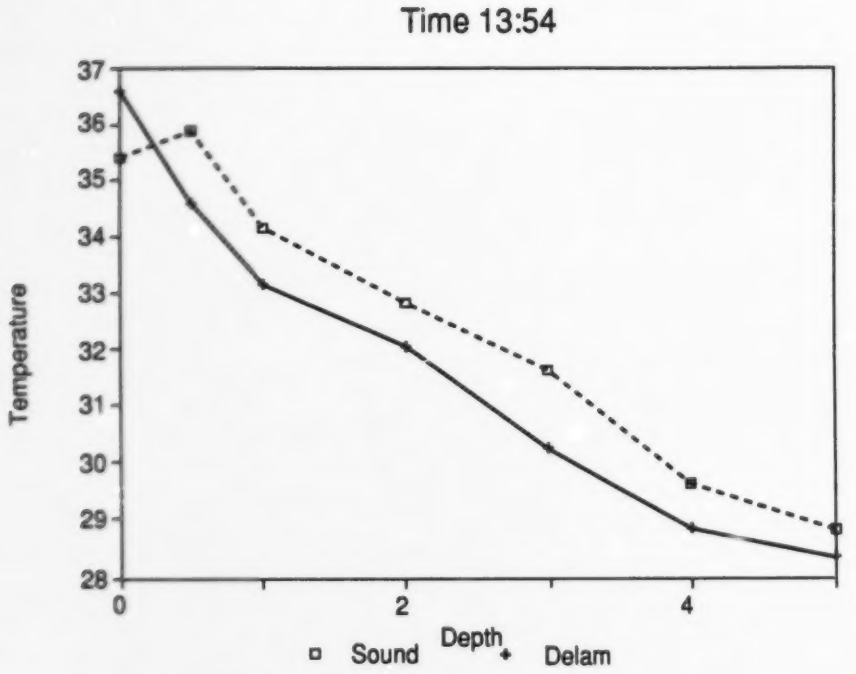

Figure 13/ Infrared Image at 13:54

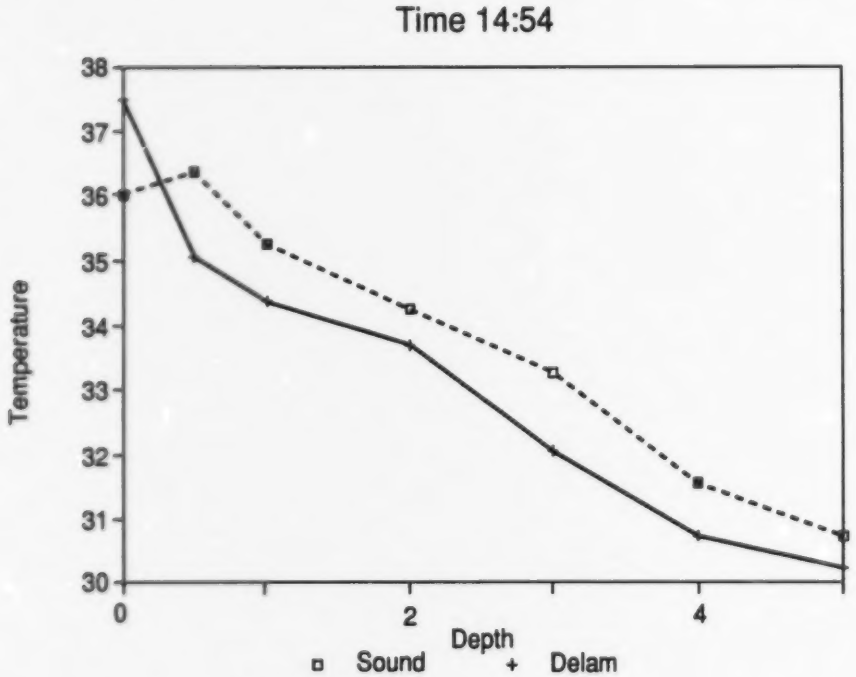

Figure 14/ Infrared Image at 14:54

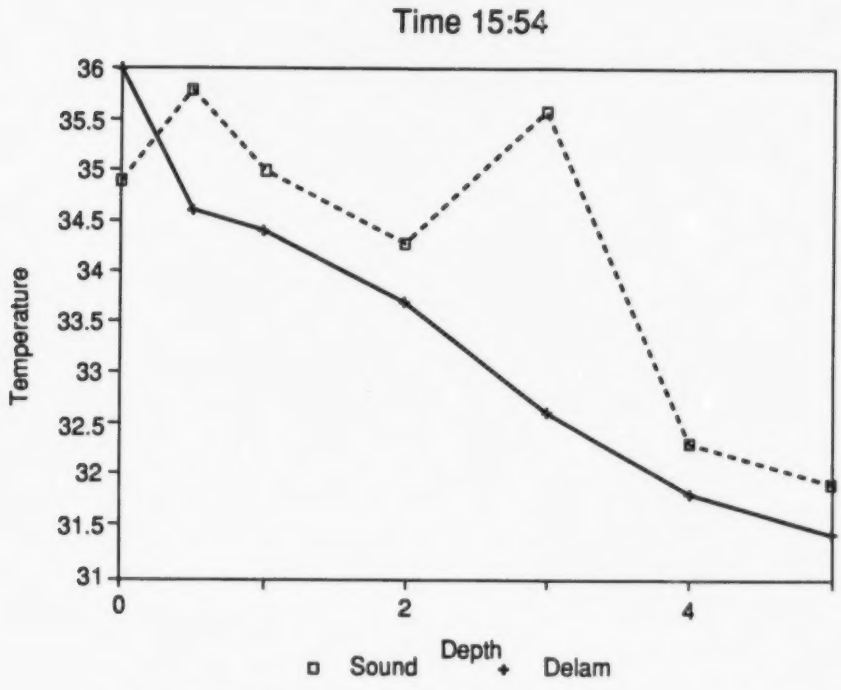

Figure 15/ Infrared Image at 15:54

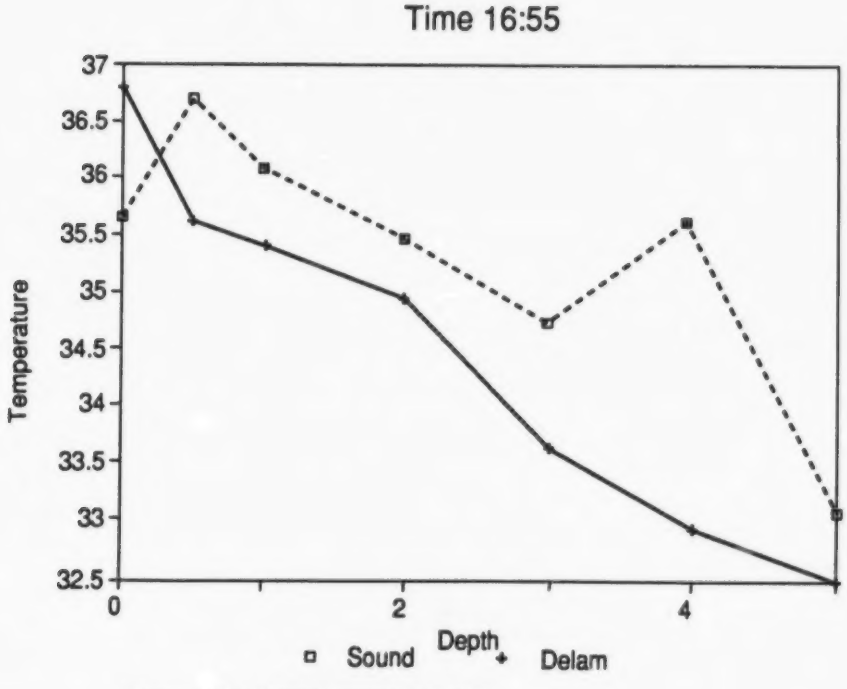

Figure 16/ Infrared Image at 16:55

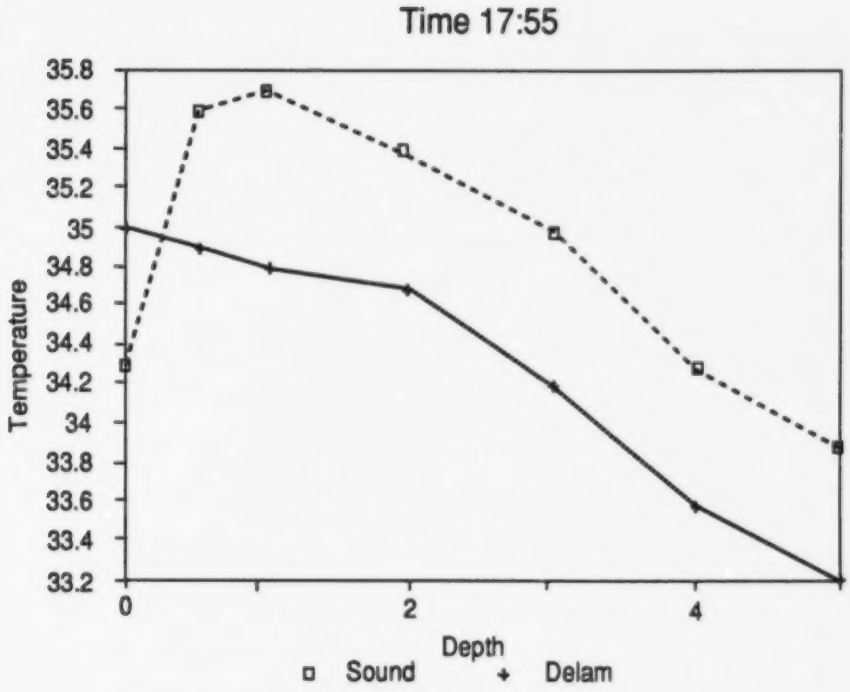

Figure 17/ Infrared image at 17:55

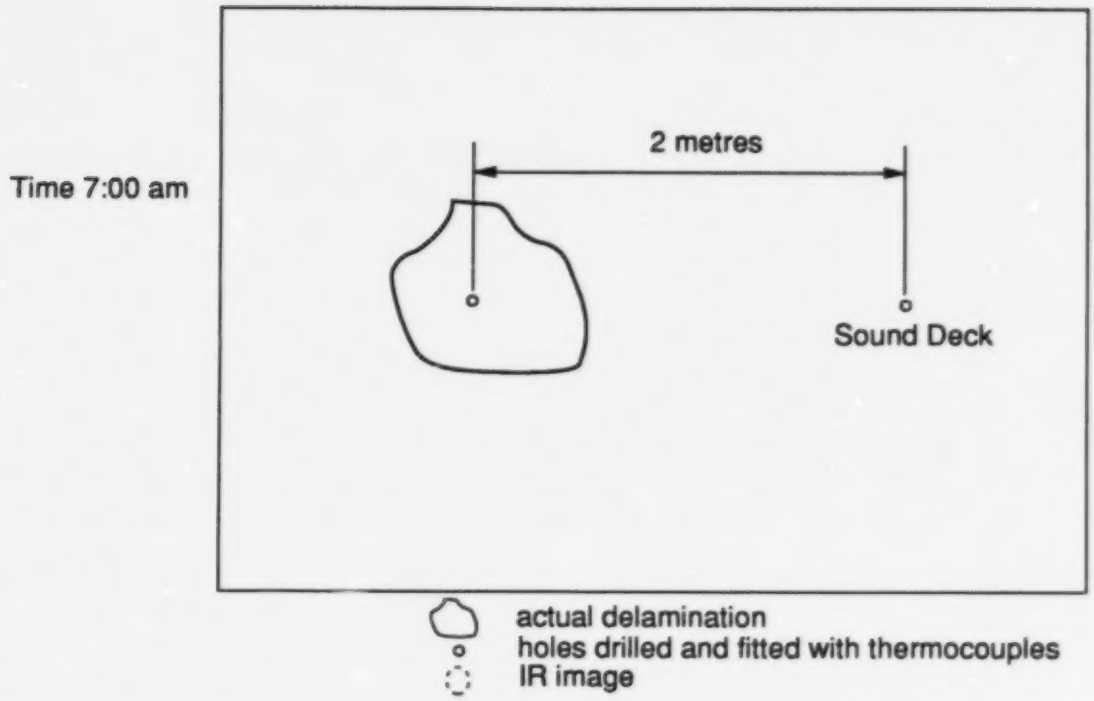

Figure 18/ IR Imaging Does Not Show a Temperature Differential

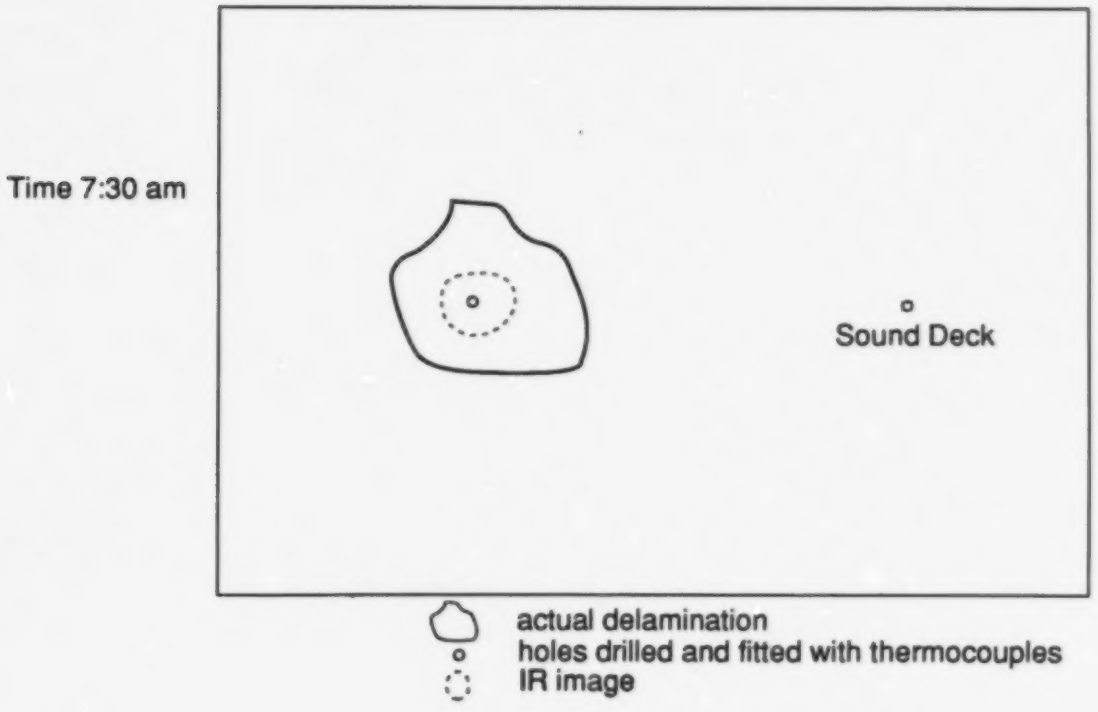

Figure 19/ Small Hotspot Visible Through Careful Gain Adjustment

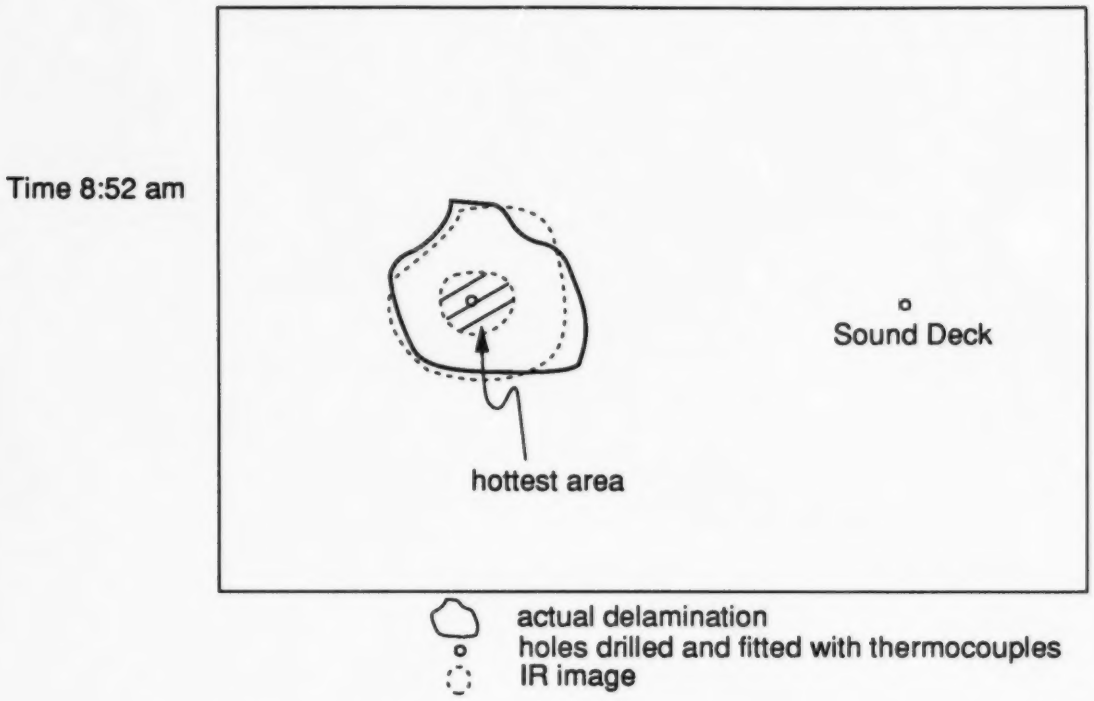

Figure 20/ Infrared Images at 8:52

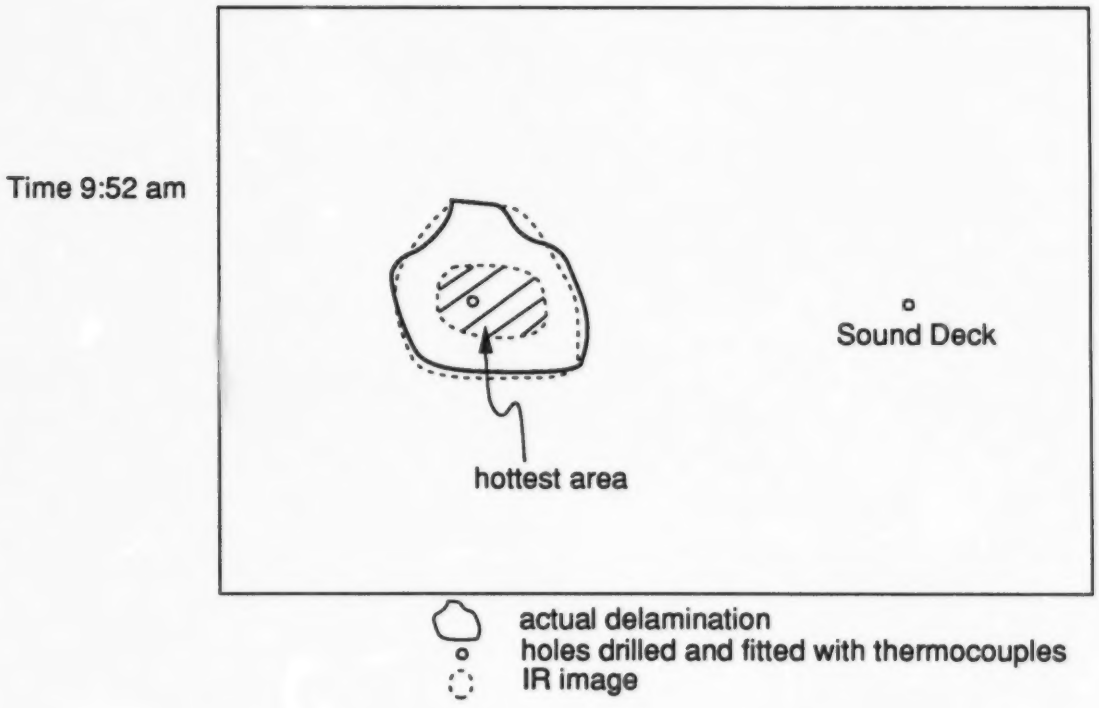

Figure 21/ Infrared Image at 9:52

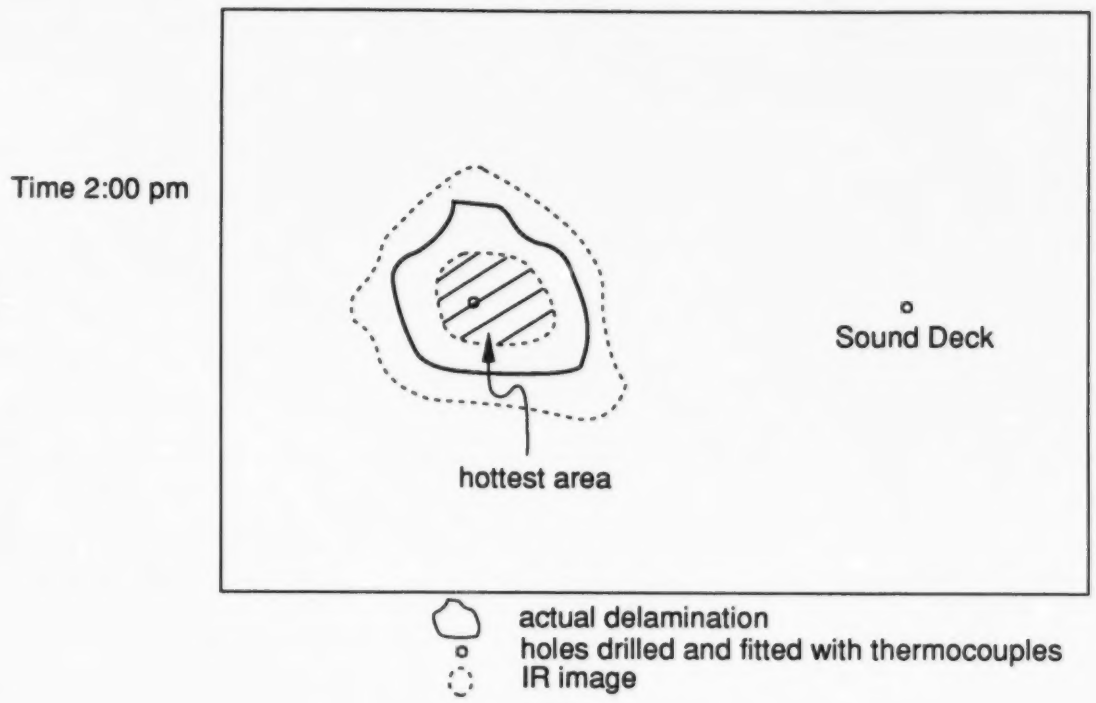

Figure 22/ Infrared Image at 2:00

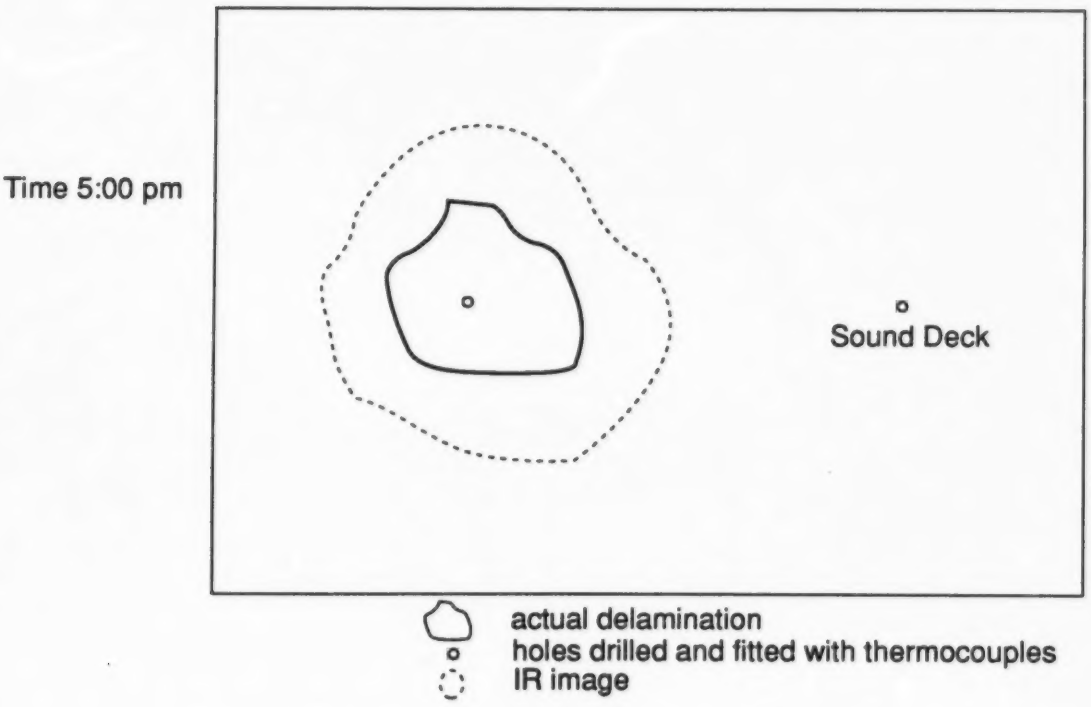

Figure 23/ Deck Temperature is Nearly Homogeneous
IR Image is Much Larger Than Actual Delamination

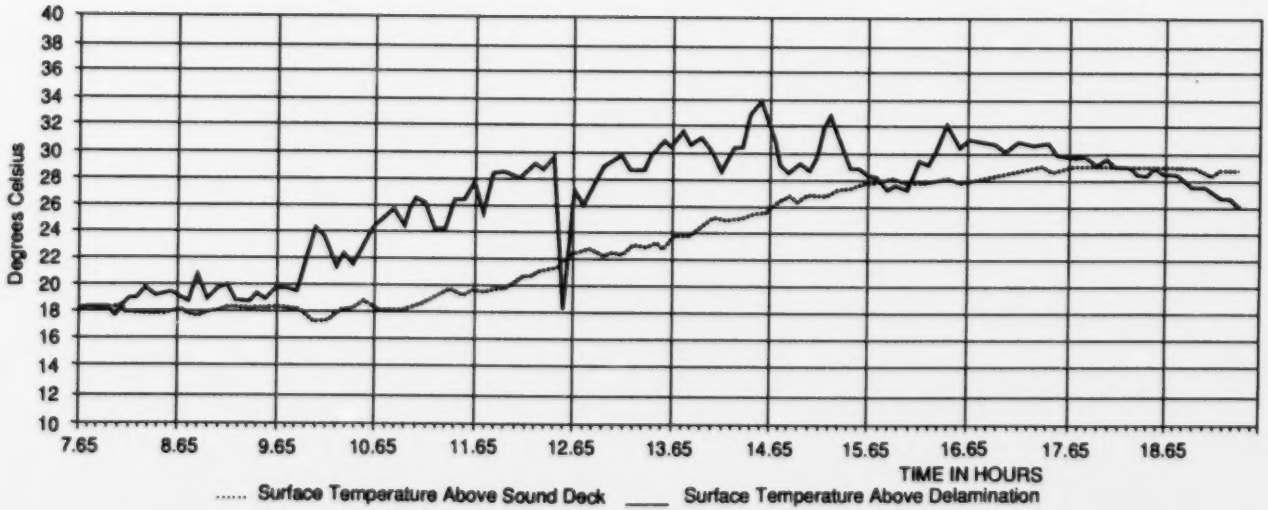

Figure 24/ Variation of Surface Temperature with Time